Study of Intermetallic Growth in Nickel Tin System Using Diffusion Couple Technique

By

C. RajaKarthikeyan

DEPARTMENT OF MATERIALS & METALLURGICAL ENGINEERING

INDIAN INSTITUTE OF TECHNOLOGY, KANPUR

DECEMBER, 1998

Study of Intermetallic Growth in Nickel Tin System Using Diffusion Couple Technique

A Thesis Submitted
in Partial Fulfillment of the Requirements
for the Degree of
Master of Technology

by

C. RajaKarthikeyan

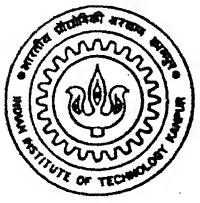

to the

Department of Materials & Metallurgical Engineering
INDIAN INSTITUTE OF TECHNOLOGY KANPUR
December, 1998

Certificate

Certified that the work contained in the thesis entitled *"Study of Intermetallic Growth in Nickel Tin System Using Diffusion Couple Technique"*, by Mr.*C. RajaKarthikeyan*, has been carried out under my supervision and that this work has not been submitted elsewhere for a degree.

Dr. S.P. Gupta
Professor,
Dept. of Materails & Metallurgical Engineering,
IIT Kanpur.

December, 1998

Abstract

Intermetallics have been of enormous, and still increasing interest in materials science and technology, with respect to applications at high temperature and a new class of structural materials is expected to be developed on the basis of intermetallics.However, it has to be noted besides intermetallics with outstanding high temperature properties, there are other intermetallics with outstanding physical properties which have given rise to development of new functional materials.

The modelisation of the formation and growth of intermetallics by interdiffusion between two metals or compounds is still a controversial field.

Diffusion couple technique was used for the study of interdiffusion phenomena between two metals.When two metals A and B are annealed at sufficiently high temperature, reactions will occur at the interface resulting in the formation of several phases between the end members. At the interface, both *thermodynamics (the equilibrium phase diagram) and the kinetics* plays an important role. The observed kinetics can be governed either by the rate of diffusion across the product phases ("diffusion control") or by the processes taking place at the interfaces ("interface control").

This work deals with the interdiffusion phenomena in *Ni-Sn* system.Diffusion couples of *Ni-Sn* have been prepared and the growth of layers formed in these couples, has been studied in the temperature range between 600^oC and 700^oC. All the phases which, on the basis of equilibrium diagram could be expected under the circumstances, were found in the diffusion zone. The layer growth of Ni_3Sn_4, Ni_3Sn_2 and Ni_3Sn obeys the *parabolic growth.* The composition range for the intermetallics has been determined from *concentration - distance profiles.*

Acknowledgments

The greatest debt of gratitude, I reserve for Prof. S. P. Gupta who guided me at every stage of this project with his perspicacious suggestions, whose qualities have attracted me a lot. I thank the almighty for giving such a brotherly figure as my guide.

I express my heart-felt thanks to all the faculty members for teaching the principles in most exciting and enjoyable way. I wish to thank my old teachers Prof. V. M. Periyaswamy, Prof. E. Ramaswamy and Mr. P. M. Kavimani for being the source of inspiration for me. I wish to express my gratitude to Dr. M. N. Mungole, Mr. Awasthi, Mr. Srivastava, Mr. R. P. Singh, Mr. Mukherjee and Mr. Sakthi Shankar for helping me out in crucial situations.

I am greatly indebted to my MTech friends Babu, Bala, Dhanabal, Gomes, Joye, Murali, Ramaswamy, Rajesh, Senthan, Venkat and all my BTech friends especially Arul, Josh, Raja, Ravi, K.Senthil, V.Senthil, Venkatesan, Anandhi and Sasi for being affectionate and encouraging. I thank all my MTech97 batch-mates especially Amrita, Avinash, Badrujjaman, Bhujbal, Gopinath, Partha, Punya, Rajeev, Sarbajit and Somnath for their exciting company. Finally, I wish I could express my thankfulness in words, to my parents and my family for their love and affection I have been receiving.

Contents

List of Tables

List of Figures

Chapter 1

Introduction

The formation of phases or compounds by interdiffusion between two elements or compounds has an important bearing on many metallurgical processes, such as *surface treatments and coatings (aluminides, silicides, Zn galvanization, tinning), high temperature corrosion, diffusion welding, composite materials, soldering of printed circuit boards and the recently found thin film contact technology.* At the *liquid-solid interface*, the growth of intermetallics occurs simultaneously with the reaction of dissolution of the solid into the liquid when it is *thermodynamically* possible.A number of studies were made on the dissolution kinetics and growth kinetics of Fe-Zn, and Nb-Sn. But very few work is done on *Ni-Sn* system, although this is one of the common interfaces used in electron devices because of the low solubility of Ni in Sn at the soldering temperatures. *Ni-Sn* system also has found application in thin film contact technology. In the *Ni-Sn* system as shown in *phase diagram* (Figure 1), three intermetallic compounds are present,

Ni_3Sn_4 $\Rightarrow$ Sn rich phase which will form first in the diffusion couple, having melting point of 795^oC.

Ni_3Sn_2 $\Rightarrow$ This is the middle phase which is stable upto 1250^oC.

Ni_3Sn $\Rightarrow$ This is Ni rich phase which is stable upto 800^oC.

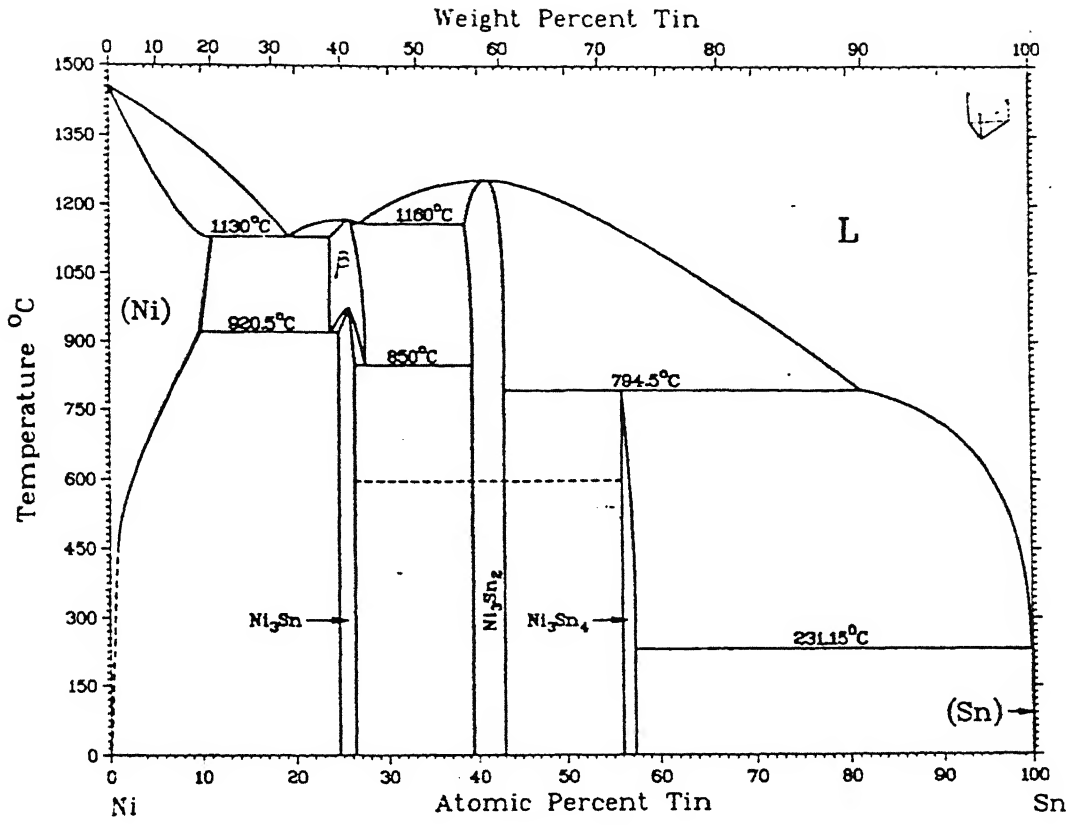

Figure 1: *Ni-Sn Phase Diagram*

The formation and growth of these intermetallics were influenced by the parameters *time and temperature*. By varying these parameters during heat treatment, we can study the kinetics of formation and growth of the intermetallics. *Diffusion couple technique* was chosen in which diffusion couples, consisting of combination of the pure metals and intermetallic compounds were subjected to heat treatment at various temperatures and subsequently examined.Using this technique, it was possible at same time to collect important diffusion data which govern the interdiffusion behavior in the *Ni-Sn* system.

Earlier,*Kang et al.*[14] studied the growth kinetics of *Ni-Sn intermetallics* by dipping the *Ni* strips in molten *Sn* bath, in the temperature range between $300°C$ and

520^oC.They showed that Ni_3Sn phase does not nucleate below 520^oC upto $8hours$ annealing time.

Van beek et al.[26] studied the phase relations and diffusion phenomena in *Ni-Sn* systems, using marker experiments. He had shown that in the case of Ni_3Sn_2 and Ni_3Sn, layer growth occurs by bulk diffusion process.

Recently, *Bader et al.*[1] has done some work related to new interconnection technology, which is based on the rapid formation of intermetallic compounds composed of a high melting component (Ni) and a low melting component (Sn) between the two layers of high melting component (Ni) at temperatures just above the melting point of Sn.

In our work, we studied the formation and growth kinetics of *Ni-Sn intermetallics* at the *solid-liquid interface* in the temperature range between 600^oC and 700^oC at various time range between 36 *hours* and 100 *hours*. The results were interpreted.

1.1 Diffusion Couple

When two metals or alloys are brought into intimate contact at elevated temperatures, interdiffusion takes place and the growth of intermetallic compounds can occur.

The number and composition of the intermetallic compounds that will grow is determined by the phase diagram, assuming quasi equilibrium. The kinetics of the formation of intermetallic compounds also plays a major role in determining the structure of the interface.

1.2 Binary Diffusion Couple

When two metals A and B are brought into intimate contact at elevated temperatures, the A and B atoms diffuse into each other. The isothermal section of the phase diagram at that temperature is applicable in determining the intermetallic layers that will form.

The single phase region in the phase diagram form phase fields, while the two

phase regions form the interface.

These interfaces move with increase in time. Due to this an equilibrium phase start growing and the other phases start diminishing. The equilibrium phase is decided by the amount of solute present in the diffusion region. Finally, only these equilibrium phases will remain in the diffusion couple.

This is possible only if we allow diffusion for sufficient time, so that metal A diffuses across the entire metal B and vice-versa.

These phases would transform into a variety of phases upon cooling as predicted by the phase diagram.

In the case of lower timings where these metals are not able to diffuse across each other, the isothermal section of the phase diagram is considered and the phases across it formed. Upon cooling, a mixture of other phases would be formed. This is a very simple way of characterizing binary diffusion couple. Some phases may not be visible in the diffusion couple due to slower growth rate even though they might have formed as a very thin layer.

As an example, consider the *Ni-Sn phase diagram* shown in Figure 2.

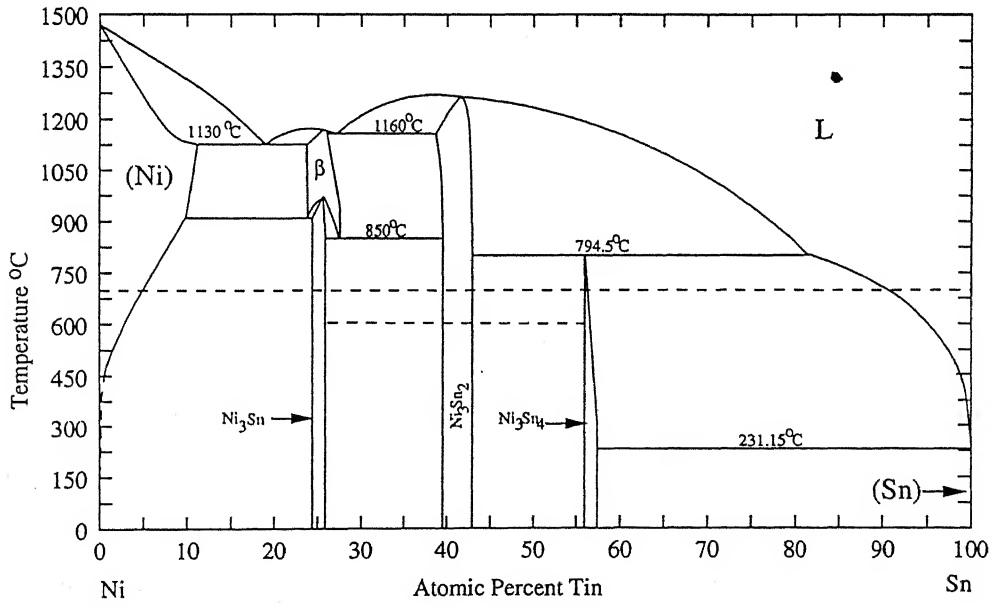

Figure 2: *Ni-Sn System at 700°C*

According to this diagram at 700^oC, we expect the diffusion couple to have the composition as shown in the Figure 3.

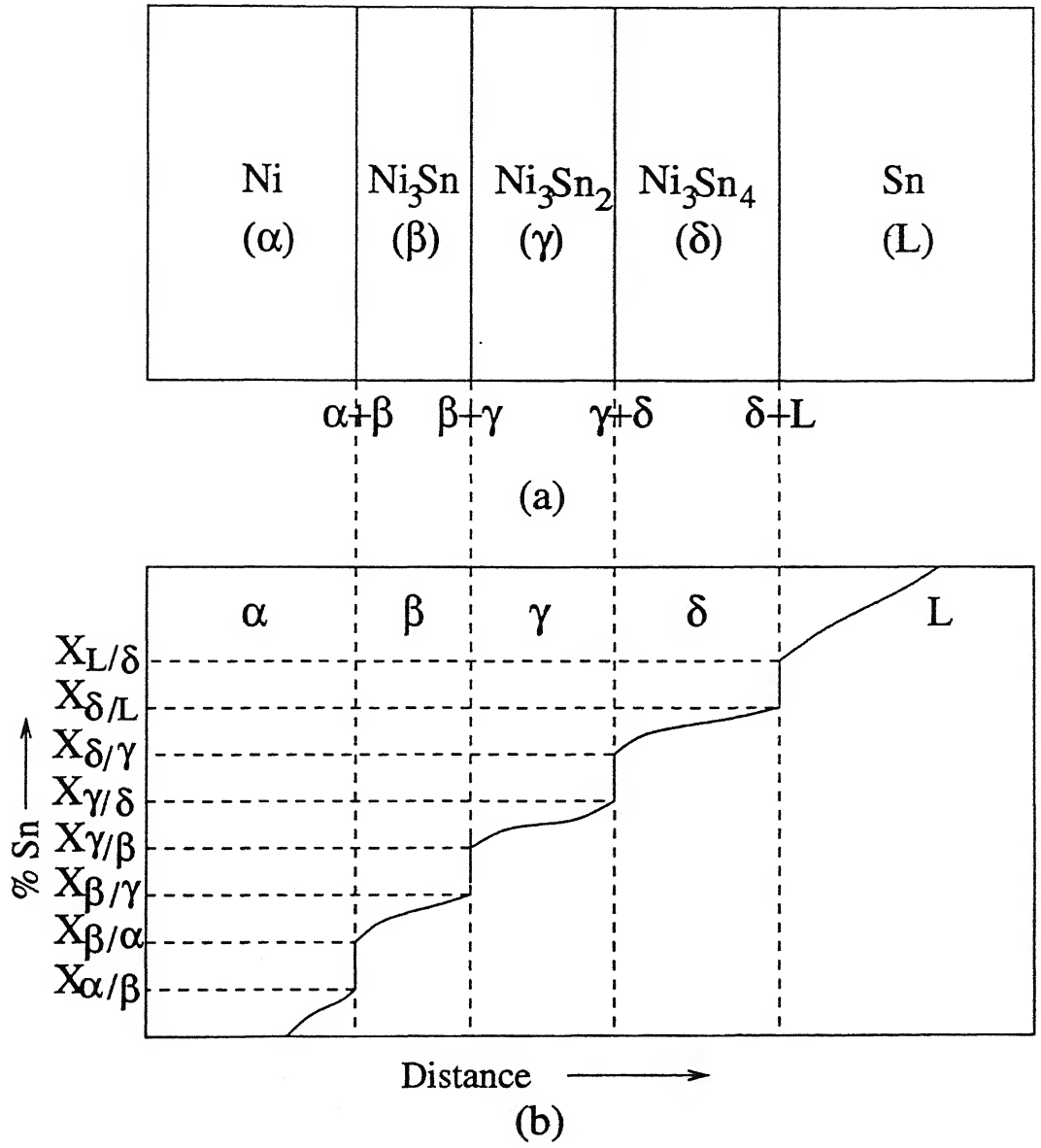

Figure 3: (a).*Ni-Sn* diffusion couple at 700^oC ; (b).Concentration - distance profile.

The diffusion couple will show four interfaces $Ni(\alpha) + Ni_3Sn(\beta)$, $Ni_3Sn(\beta) + Ni_3Sn_2(\gamma)$, $Ni_3Sn_2(\gamma) + Ni_3Sn_4(\delta)$ and $Ni_3Sn_4(\delta) + Sn(L)$ as shown in Figure 3.

The concentrations of Ni and Ni_3Sn at the Ni/Ni_3Sn interface are shown as $X_{\alpha/\beta}$

and $X_{\beta/\alpha}$. The concentrations of Ni_3Sn and Ni_3Sn_2 phases at the Ni_3Sn/Ni_3Sn_2 interface are shown as $X_{\beta/\gamma}$ and $X_{\gamma/\beta}$. The concentrations of Ni_3Sn_2 and Ni_3Sn_4 phases at the Ni_3Sn_2/Ni_3Sn_4 interface are shown as $X_{\gamma/\delta}$ and $X_{\delta/\gamma}$. The concentrations of Ni_3Sn_4 and $Sn(L)$ at the $Ni_3Sn_4/Sn(L)$ interface are shown as $X_{\delta/L}$ and $X_{L/\delta}$.

In the case, when one of the member becomes liquid, the above assumption of semi infinite bodies is not valid, because the diffusivity of the metals in liquid is more than that of solid.The diffusion of Ni occurs rapidly across the entire layer of liquid Sn.An estimation and measurements by *Toshima et al.*[25] shows that the saturation time is between 1 and 3 s. Due to this, a gradient sets up in the liquid. The new concentration profile is shown in Figure 4.

The structure of the profile may change due to the freezing of the liquid with gradient or due to certain phases occupying the liquid part of the diffusion couple.

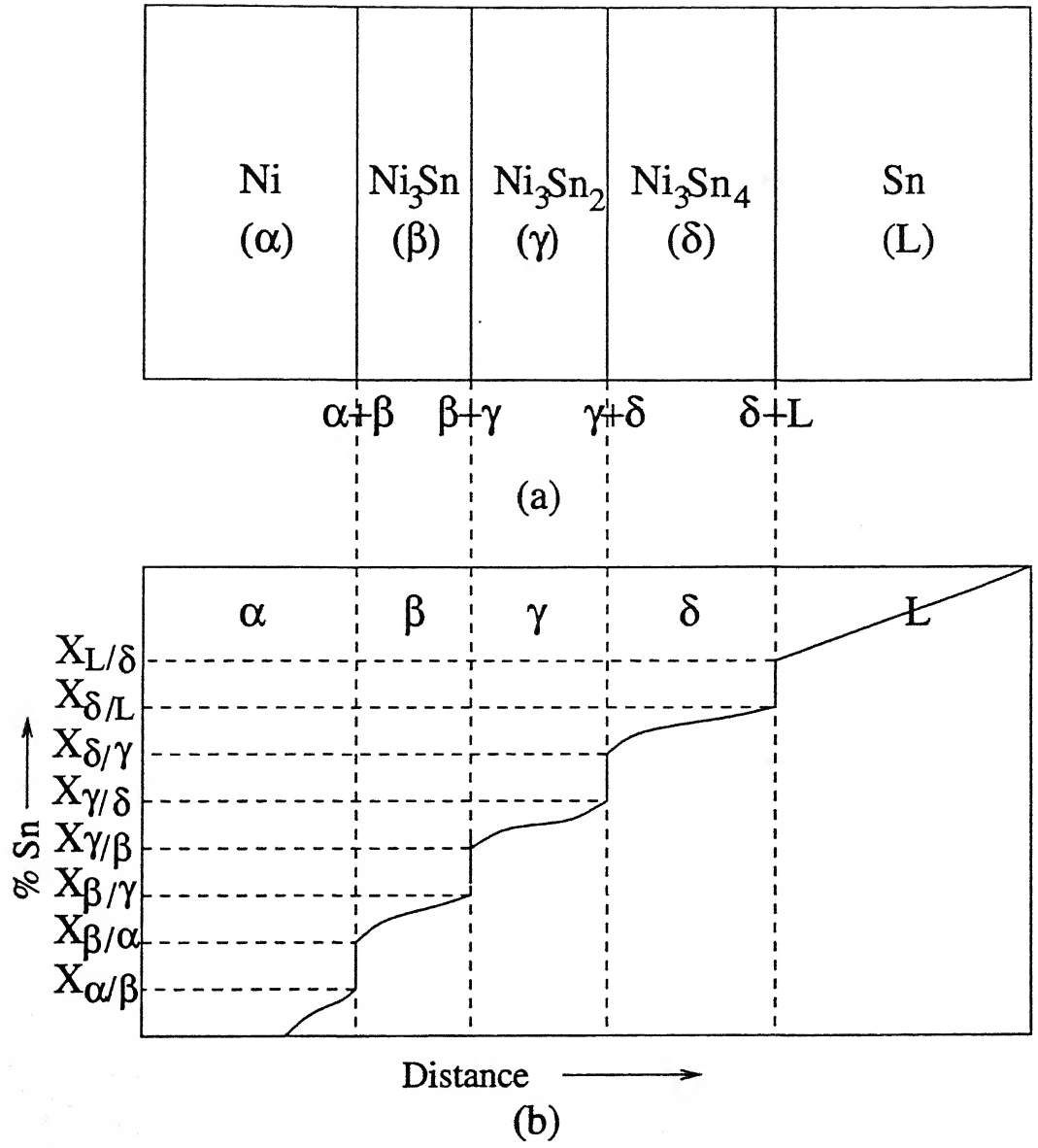

Figure 4: (a) *Ni-Sn* diffusion couple after liquid *Sn* homogenization at $700°C$; (b). Concentration - distance profile

Chapter 2

Literature Review

2.1 Evolution of phase growth in diffusion couples

Let us consider a diffusion couple A/B between two metals A and B. By an appropriate annealing, one expects to observe the formation of all the phases stable at this temperature according to the equilibrium phase diagram. All the intermediate phases would appear in the couple as a series of parallel layers whose thickness will be increasing with time of annealing as shown in Figure 5.

The growth kinetics of a single compound layer is determined by a combination of two types of *physico - chemical processes*,

- The diffusion of matter across the compound layer where the diffusion flux slows down with layer thickness.
- The rearrangement of the atoms at the interfaces required for the growth of the compound layer which may involve a reaction barrier.

If the diffusion process is rate limiting and controls the growth, the corresponding kinetics is termed *diffusion controlled* and the layer thickness is proportional to the square root of time. If the interfacial reaction barriers controls the kinetics, it is termed *interface controlled* and the layer thickness increases linearly with time.

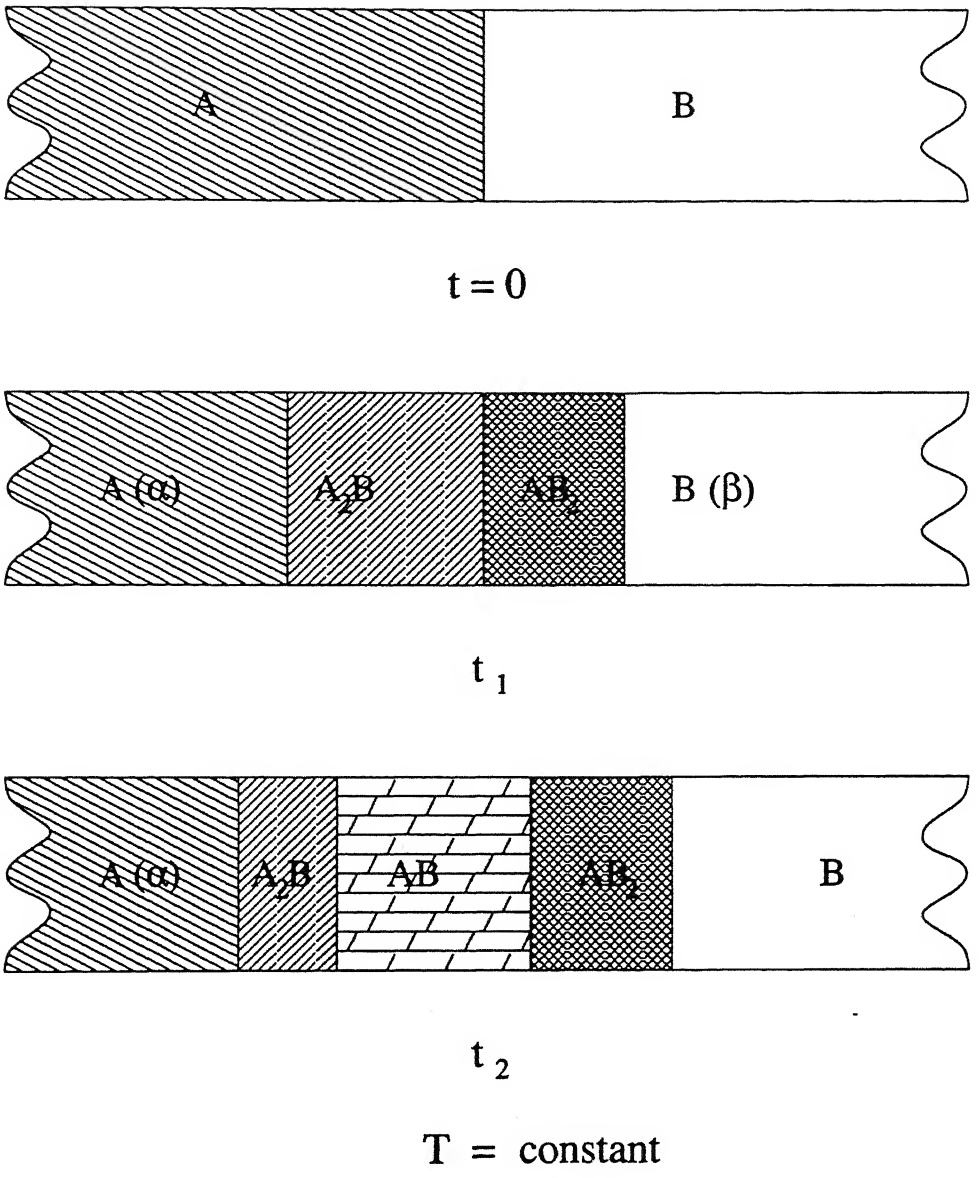

Figure 5: Evolution of phase growth in infinite diffusion couple.

2.2 Nucleation of an intermediate compound

The nucleation of an intermediate compound in this case is different from the classical nucleation process in a homogeneous supersaturated solution, because we are dealing with the formation of a new phase along a planar interface of infinite extent [17]. Let γ_1, γ_2 and γ_3 be the interfacial energies (per unit area) of the initial interface and

of the two interfaces created by the formation of a new phase of layer thickness ξ, of the new phase (Figure 6).

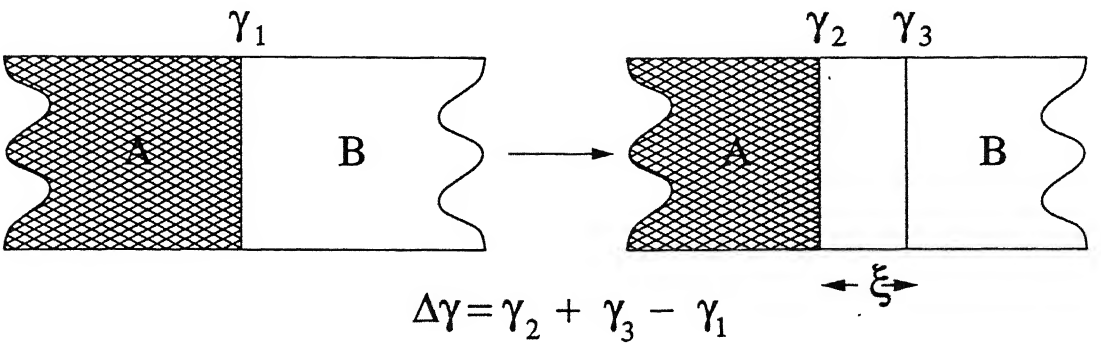

Figure 6: Formation of an intermediate phase.

The change in Gibb's free energy per unit area is given by :

$$\Delta G = \xi \Delta g_v + \Delta\gamma \tag{1}$$

where $\Delta\gamma = \gamma_1 + \gamma_2 + \gamma_3$ and Δg_v the free energy driving the phase transformation (Figure 7).

- if $\Delta\gamma < 0$, ΔG will be negative and decrease continuously as ξ increases, there is no critical condition for nucleation.
- if $\Delta\gamma > 0$, there exists a critical thickness $\xi^* = \Delta\gamma/\Delta g_v$, above which ΔG is negative. Therefore, a heterogeneous process is then possible with nuclei localized on certain sites at the interface [10][17].

It has been found that there are some lack of correspondence between the equilibrium phase diagram and the phases appearing in diffusion zone:

- Only part of the phases present in equilibrium diagram are appearing.
- In some systems new metastable phases appear which are absent in the equilibrium phase diagram. For example in Ni-Zr, Au-La systems.

There are two alternative explanations for these anomalies. They are:

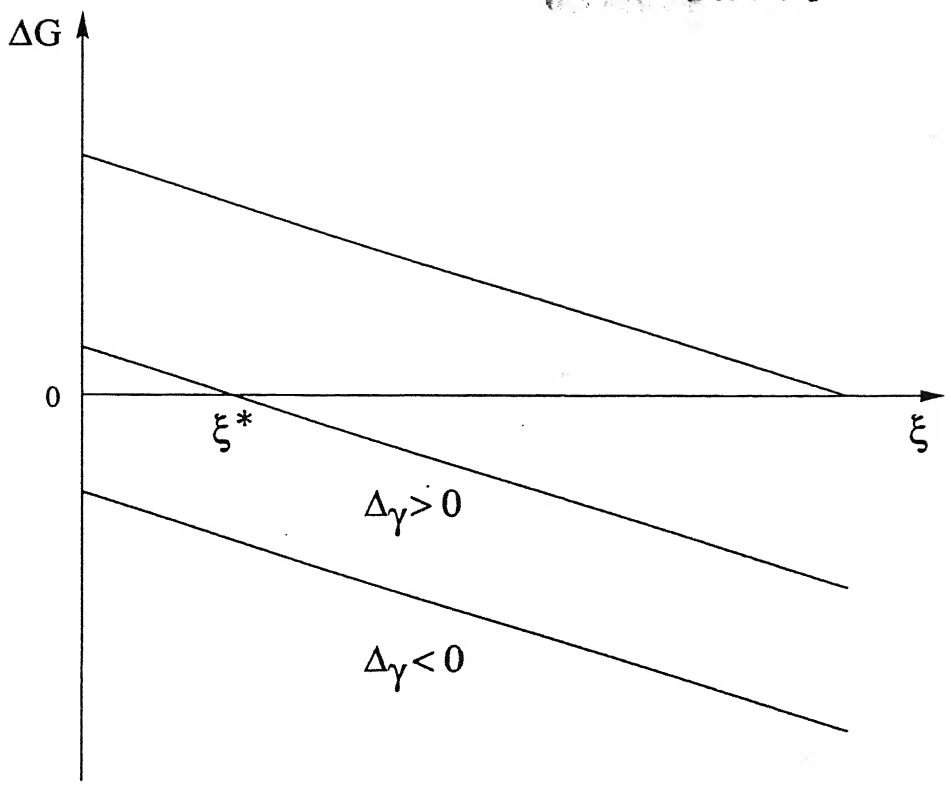

Figure 7: Gibb's free energy for the formation of an intermediate phase.

1. The explanations given by *Gösele and Tu [12], Dybkov [6] [7] [8].* It takes into account the reaction barriers on the moving interfaces.

2. The explanations given by *Gusak et al.[13].* It takes into account the difficulties of nucleation in the field of concentration gradient and the diffusional interactions on the nucleation stage.

2.2.1 Effect of concentration gradient on the intermediate phase nucleation

The theory given by *Gusak and Gurov* [13]*and Désre and Yavarí [4]* states that the nucleation of intermediate phase takes place in the field of concentration gradient and the nuclei from the very beginning take part in the diffusional interaction with parent phases and with the nuclei of other intermediate phases. For the nucleation of an

intermediate phase, there must exist some preferred region with such concentrations which are favorable for a new phase (Figure 8). The nucleation process progresses through two stages:

1. The formation of new metastable solution from the parent phases.
2. The nucleation of new phase in the meta stable solution at some preferred regions.

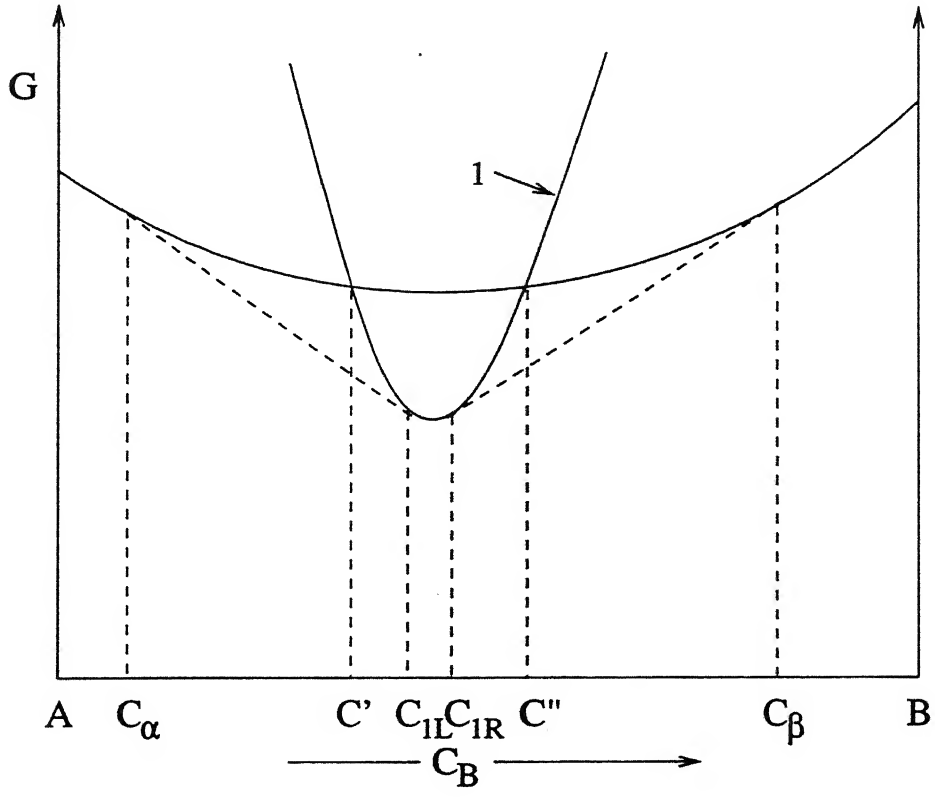

Figure 8: Gibb's free energy as a function of concentration C in a binary system with metastable parent solution and intermediate phase 1.

The corresponding change of Gibb's free energy of the system in the presence of concentration gradient is given by:

$$\Delta G = v^{-1} \int \Delta g(C) S(x) dx + \sigma 4\pi R^2 \tag{2}$$

where in the case of a spherical nucleus $S(x) = \pi(R^2 - x^2)$, v is an atomic volume, $\Delta g(C)$ is the change of Gibb's free energy per atom in the process of transformation of metastable solution with concentration C into the phase 1.

The above expression can be presented in the form

$$\Delta G = \alpha R^2 - \beta R^3 + \gamma R^5 \tag{3}$$

where first two terms are *surface and volume* contributions and the last term depends on the concentration gradient of the parent metastable phase, $\gamma = 2\pi g"/(15vL^2)$, $L = (\partial C/\partial x)^{-1}$, $g" = \partial^2 g/\partial^2 C$, g is a Gibb's free energy per atom.

ΔG has a bifurcation at the point $L = L^* = 3R^*/\Delta_m C$, where R^* is the radius of a critical nucleus in a homogeneous alloy of composition C, $\Delta_m C$ is the concentration range within which new phase is favorable than the parent one.

- At $L < L^*$, ΔG increases with R, nucleation is thermodynamically unfavorable.
- At $L > L^*$, the dependence of ΔG becomes nonmonotonous (Figure 9) and the nucleation becomes thermodynamically possible in the range $R_1 < R < R_2$, R_2 growing to infinity together with L.

2.2.2 Nucleation of next intermediate phase and further phases

Once a phase ζ, which does not require critical conditions for nucleation is formed, it is quite possible that the driving free energy Δg_v for the next intermediate phase η becomes very small. This is shown in an isothermal diagram of the free energy curves of the different intermediate phases plotted as a function of the compositions of the system (Figure 10).

This would result in a high value of ξ^*, and eventually some difficulty for nucleating η phase, which can then appear when temperature is raised sufficiently [5].

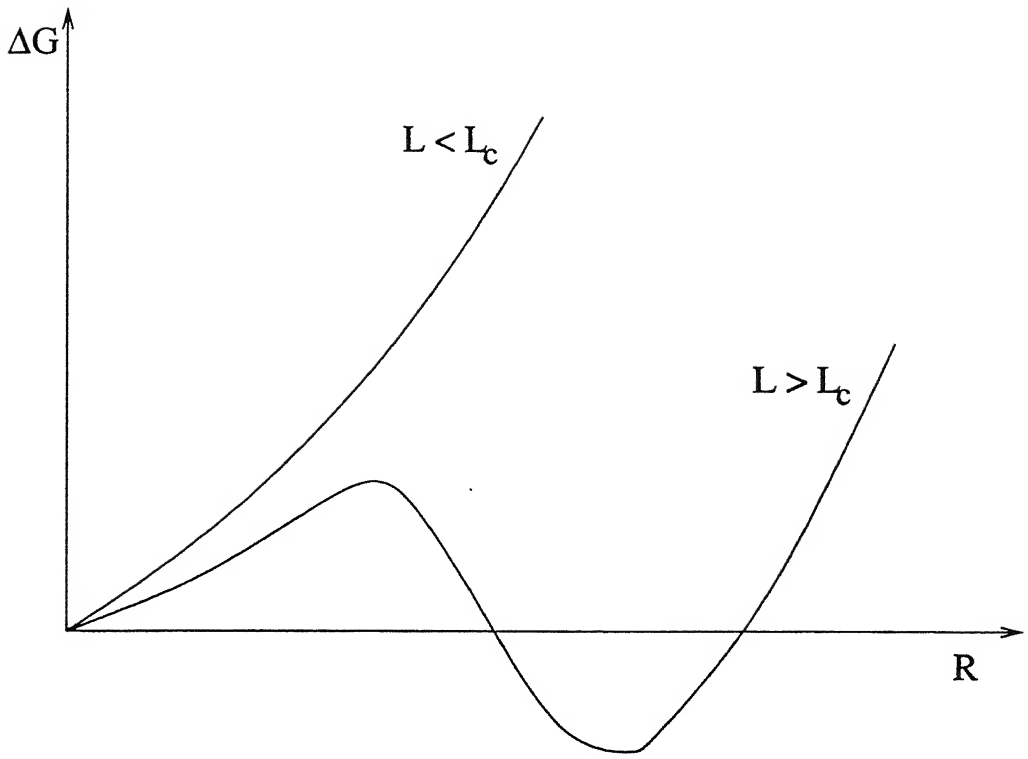

Figure 9: Change of Gibb's free energy as a function of nucleus size: case of spherical nucleus in the field of concentration gradient

2.3 The Kinetics of phase growth

In the case of diffusion controlled process, the derivation of the time schedule $\xi\ (t)$ of an interface between two phase in an interdiffusion couple A/B is a simple problem. Let us consider the application of Fick's first law to a diffusion couple made up of two pure metals which have limited solubility in the primary phases and no intermediate phases. Figure 11 shows the concentration profile and corresponding equilibrium phase diagram.

Assuming the concentrations at the interface as constant (i.e. the equilibrium values) and considering the flux of material from left to right, the rate of advance of the interface at $\xi_{\alpha\beta}$ is given by

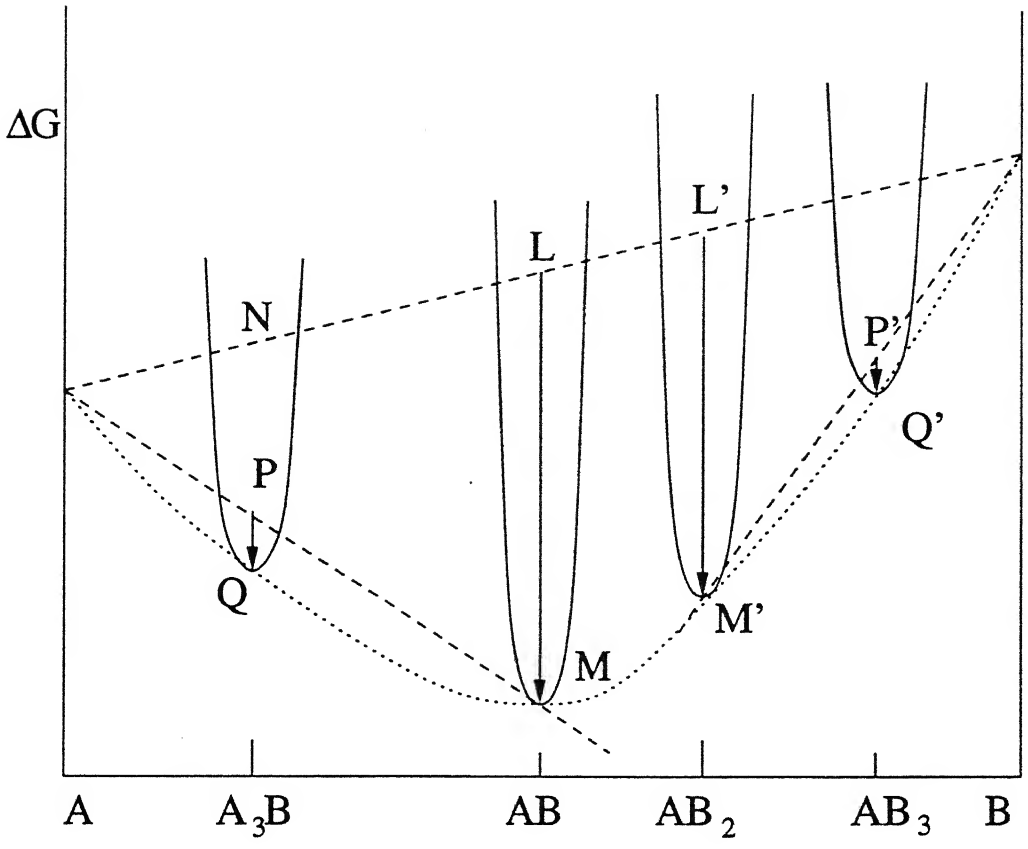

Figure 10: Gibb's free energy curves for a series of compounds in a binary system.The driving force for a second phase (PQ or P'Q')is smaller than for the first one(LM or L'M').

$$(C_{\alpha\beta} - C_{\beta\alpha})\frac{d\xi_{\alpha\beta}}{dt} = -D^{\alpha}\left(\frac{\partial C}{\partial x}\right)_{\alpha\beta} + D^{\beta}\left(\frac{\partial C}{\partial x}\right)_{\beta\alpha} \tag{4}$$

The left hand side represents the change in the number of diffusing atoms due to the growth of β phase and the right hand side is the difference in the fluxes of this species just at the left and at the right of the interface.

Applying Boltzmann theorem to the above system, the concentration $C(x,t)$ can be expressed as a function of a single parameter $\lambda = x/\sqrt{t}$, and from this we can write,

$$\frac{\partial c}{\partial x} = \frac{1}{\sqrt{t}}\frac{dc}{d\lambda} \tag{5}$$

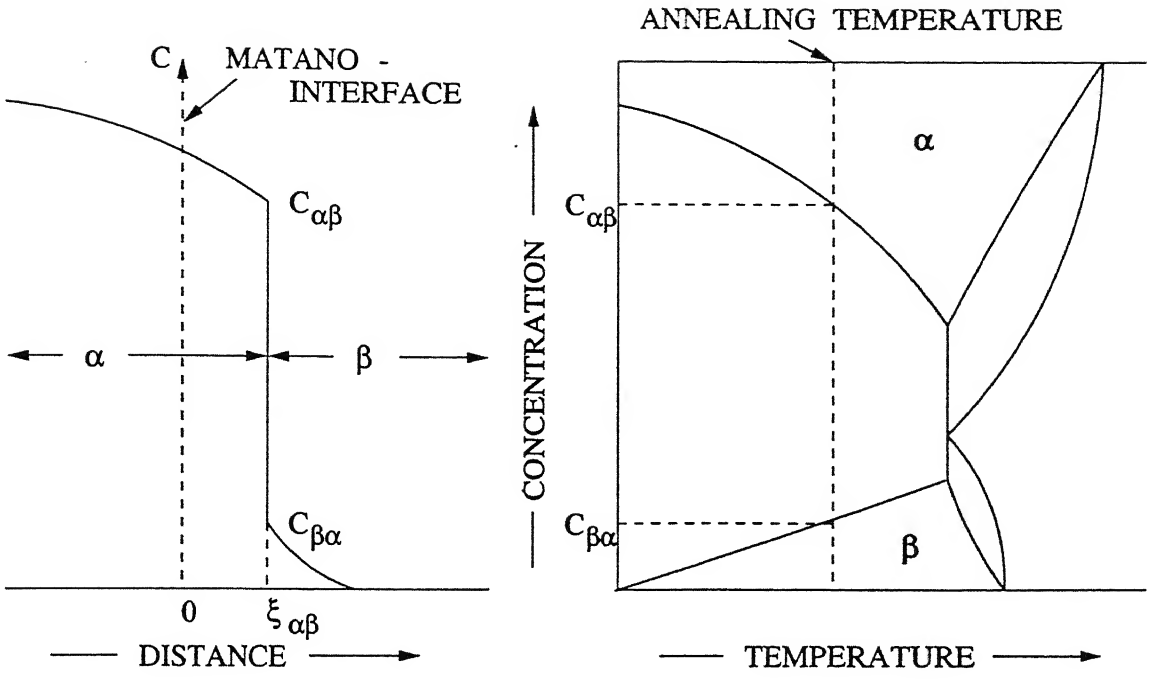

Figure 11: The relationship between the equilibrium diagram, the diffusion annealing temperature and the diffusion zone interface concentrations for a two phase system.

Equation 4 can be written as

$$\frac{d\xi_{\alpha\beta}}{dt} = \left[\frac{-(D^{\alpha}K)_{\alpha\beta} + (D^{\beta}K)_{\beta\alpha}}{(C_{\alpha\beta} - C_{\beta\alpha})}\right]\frac{1}{\sqrt{t}} \tag{6}$$

where

$$K = \frac{dc}{d\lambda} = \sqrt{t}\left(\frac{\partial c}{\partial x}\right) \tag{7}$$

Solving the equation 6 gives,

$$\begin{aligned} \xi_{\alpha\beta} &= 2\left[\frac{-(D^{\alpha}K)_{\alpha\beta} + (D^{\beta}K)_{\beta\alpha}}{(C_{\alpha\beta} - C_{\beta\alpha})}\right]\sqrt{t} \\ &= A_{\alpha\beta}\sqrt{t} \end{aligned} \tag{8}$$

As a similar equation applies to the next interface β/γ, the growth of the β phase will follow a parabolic time schedule :

$$\Delta\xi_\beta = \xi_{\beta\gamma} - \xi_{\beta\alpha} = (A_{\beta\gamma} - A_{\alpha\beta})\sqrt{t} \tag{9}$$

These are the mainlines of the classical treatment given by *Kidson*[17]. By considering the role of the processes occurring at the interfaces, the equation becomes different.

For the progress of reaction at the interface needs super saturation, i.e. change in equilibrium : $C_{\alpha\beta} \neq \overline{C}_{\alpha\beta}$. Then the growth rate equation becomes :

$$\Delta\xi^2 + \frac{2\mathcal{D}}{\kappa}\Delta\xi = 2\mathcal{D}(t - t_o) \tag{10}$$

where,

- $\mathcal{D} \Rightarrow \mathcal{D}_B(C_{\beta\gamma} - C_{\beta\alpha})$
- $\kappa \Rightarrow \kappa_{\alpha\beta}(C_{\alpha\beta} - \overline{C}_{\alpha\beta})$

This kinetic equation simplifies for two cases,

1. For short times ($\mathcal{D} \gg \kappa$),

$$\Delta\xi \propto t - t_o \tag{11}$$

This linear region is known as *interface controlled region.*

2. For longer times ($\mathcal{D} \ll \kappa$),

$$\Delta\xi \propto (t - t_o)^{\frac{1}{2}} \tag{12}$$

i.e. parabolic region. This is said to be as *diffusion controlled region.*

With increasing time a transition from linear region to parabolic region is expected for

$$\Delta\xi^* = \frac{2\mathcal{D}}{\kappa} \tag{13}$$

The above derivation of the parabolic law is first done by *Evans*[9] and later *Deal and Grove*[3] rediscovered the same in their theoretical work.

In the case of formation of the next phase, the interface and reactions will be different and the growth kinetics will be different.*Dybkov*([6][7][8]) has shown the differences in the growth kinetics for a given A/B system according to the nature of the neighbouring phases. eg. $A/\ \beta\ /B$ or $A/\ \beta\ /\ \zeta\ /B$.

The second phase AB will not grow until phase A_2B has reached a *critical thickness (Gösele and Tu [12], Gösele [11])* whose magnitude increases when

- Diffusivity through A_2B is larger.
- The interface rate constant of AB is smaller.

In an infinite couple the AB phase will start to grow between A_2B and B after some delay time (or "incubation" period) unless B has been exhausted (finite couple) (Figure 12).

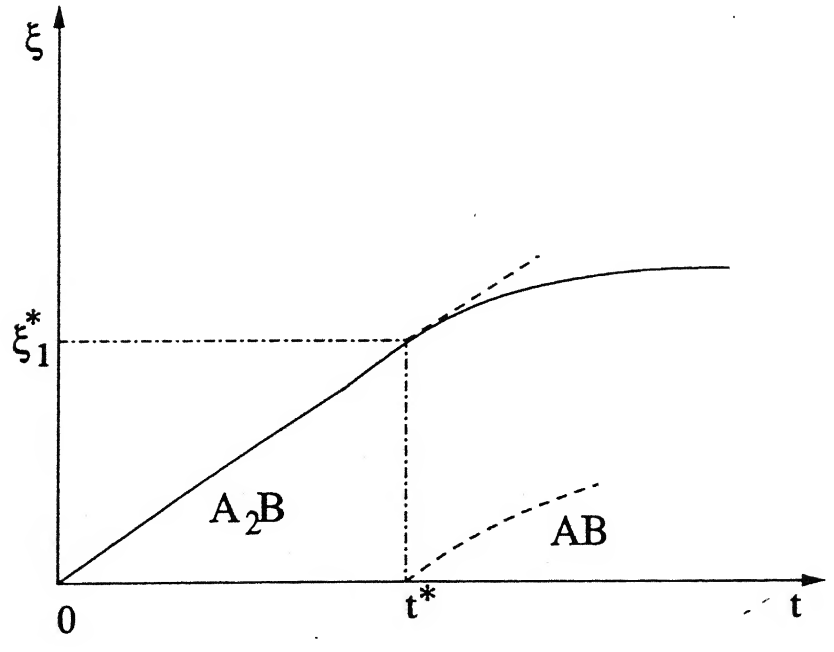

Figure 12: Critical thickness for the growth of second compound.

2.4 Grain boundary diffusion

The intermediate layers may grow as single crystals, but in most cases it is polycrystalline. Their microstructure shows that these grains are columnar, with their long axis along the direction of the diffusion flux. Hence, the atomic transport along the boundaries is also taken into consideration for diffusion coefficient calculation.

The effective interdiffusion coefficient D_{eff}, is the weighted average of the bulk diffusion coefficient D and the grain boundary diffusion coefficient D_{gb}[22].

$$D_{eff} = D + a \frac{2\delta}{d} D_{gb} \tag{14}$$

where

d $\Rightarrow$ average grain diameter.

δ $\Rightarrow$ thickness of the grain boundary.

a $\Rightarrow$ shape constant ($a \approx 1$).

As the grain size decreases, D_{eff} will increase, because $D_{gb} \gg D$. Both the bulk and grain boundary diffusion coefficients, as well as the grain size are temperature dependent and increase with increasing temperature [21].

Therefore, the activation energy is not a true constant.

2.5 Effect of stress on diffusion

During interdiffusion in a binary system, the components have different atomic volumes (or) different mobilities, a resulting "volume" transport (or) atomic (vacancy) current may arise. This leads to inhomogeneous deformation (stress - free strain), on one side of the diffusion couple contractions while on the another side extensions will arise [24].

Since different regions of the diffusion zone are coupled elastically, internal stresses arise during interdiffusion. These internal stresses contribute to the driving forces of

the atomic currents and plastic deformation. The plastic deformation tends to relax the stress generated by diffusion and the overall deformation produces convective transport. These convective terms should be included into the treatment of interdiffusion [2].

2.6 Kirkendall Effect

Two components may diffuse at unequal rates in opposite directions across their common interface in association with a flux of vacancies [23]. This gives rise to the *kirkendall effect* [18] which is revealed by the movement of inert marker at this interface.The direction of the vacancy flux is generally towards the component of lower melting temperature and the eventual behavior of these vacancies can be complex. They can be absorbed at grain boundary sinks or at dislocations by causing them to climb. Alternatively, the vacancies may climb and agglomerate and condense to form voids [16].

2.7 Determination of interface movement using markers

The movement of A/B interface in a diffusion couple between A and B can be determined by placing inert markers at the interface. This interface is normally called as *kirkendall interface.*

If A atoms diffuse fast then the interface moves towards B side and vice-versa. The relative mobilities of both A and B can be determined.

Chapter 3

Experimental Setup

Nickel and *tin* both of 99.99% purity were used as starting materials.Ni samples were prepared from Ni ingots. In the Ni ingot which had a square cross section of $8mm \times 10mm$, a preliminary cut was made along the cross section using the diamond cutter to make its surface flat.Then further cuts are made parallel to the first cut to get slices of $1.5 - 2mm$ thick. These Ni slices were homogenized at $900°C$ for $24h$ under vacuum.After homogenizing, these samples were polished using standard metallographic procedure to ensure flat surface for good wettability.Sn samples of diameter $3mm$ were used.These Sn samples were also polished on one side to make the surface flat, exposing maximum area for bonding.

The parts were then cleaned ultrasonically in methanol to remove all the debris on the polished surface which could hinder bonding.Then the parts were assembled in the set up as shown in the Figure 13.

In the assembly first the rectangular slice of Ni was placed on the bottom. The metal Sn was placed on top of Ni.Since the temperature used for conducting the experiments was more than that of the melting point of pure Sn, it would be molten. They would have sufficiently high fluidity and would flow off the Ni surface.To avoid this spillage, Sn samples were placed inside the *graphite disc.* This disc was polished on both surfaces, so that there is no leakage between the disc and the metal surface. This assembly was made air tight using screw arrangements.

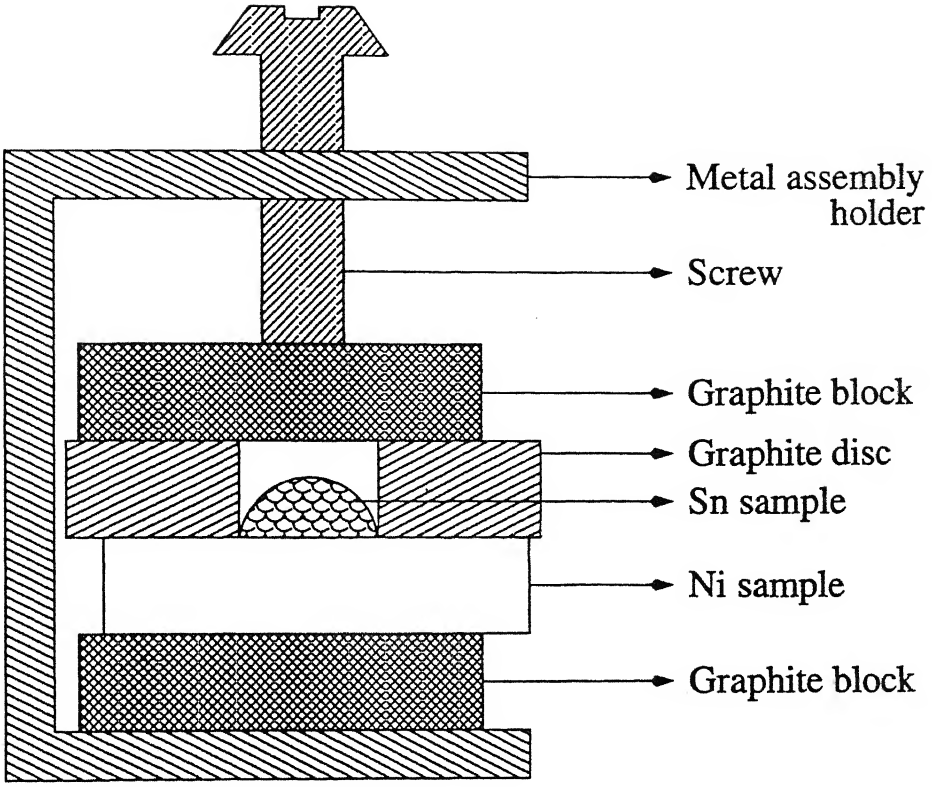

Figure 13: Diffusion couple assembly.

The assembly was then placed in a quartz tube, which was then connected to a rotary vacuum pump. The pump produces vacuum of 10^{-3} to 10^{-4} torr inside the quartz tube.The quartz tube was then placed gently inside a *vertical tube furnace*, which was maintained at a fixed temperature and annealed. The temperature used for annealing in our present case was in the range $600°C$ and $700°C$. The annealing time at each temperature varies in the range from $36h$ to $100h$.

After the annealing treatment, the diffusion couples were air cooled under vacuum to prevent oxidation. After cooling, the couples were removed from the quartz tube. A cross section was made at the interface as shown in the Figure 14.

The sample was then mounted and polished using standard metallographic procedure. The samples were then analyzed using *polarized light microscopy, Scanning Electron Microscopy (SEM) and Electron Probe Micro Analyzer (EPMA).*

For the optical microscope observations, a Ziess microscope with a magnification

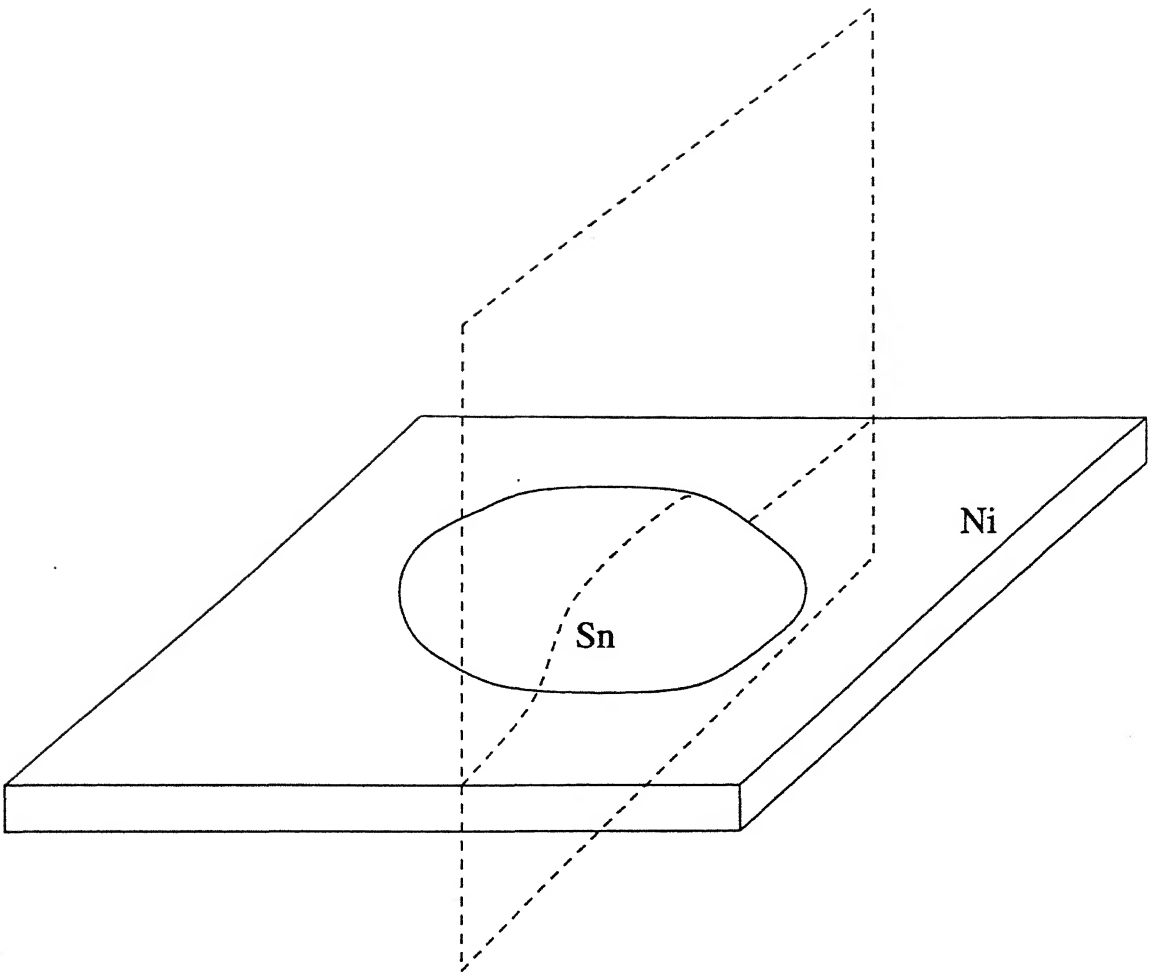

Figure 14: Cutting plane of the diffusion couple to expose interface.

of 100:1 was used . The width of the Ni_3Sn_4 intermetallic layer was measured on the screen of a video system connected to the microscope at a total magnification of 100:1.Due to the irregularity of interface, the average thickness of an intermetallic was determined by measuring the layer thickness throughout the interface at equally spaced points.

Chapter 4

Results and Discussions

The results of qualitative investigations carried out with *Ni-Sn* diffusion couples in the temperature range between 600^oC and 700^oC, were in complete agreement with the equilibrium diagram. The growth of intermetallics occurs by solid Ni - liquid Sn interdiffusion. Sn atoms from liquid will diffuse faster, as compared to Ni atoms, at the interface resulting in the growth of intermetallics towards Sn side.Ni atoms moves slowly and after sometime liquid Sn will get saturated with Ni. During the start of the reaction, liquid Sn diffusion controls the growth and later on, Ni diffusion through solid intermetallic layer controls the growth. Three intermetallic layers Ni_3Sn_4, Ni_3Sn_2 and Ni_3Sn were found to be formed.

4.1 Microstructure

The *Ni-Sn* diffusion couple interface was studied using *Scanning Electron Microscopy.*

Figure 15 shows the *Ni-Sn* diffusion couple interface treated at 680^oC for $81h$. The top portion of the micrograph is the saturated Sn solid solution with Ni. Below this is the Ni_3Sn_4 layer grown as *hemispheres. Badar et al.* [1] had shown that this layer to be exhibiting in three different morphologies simultaneously as a :

- fine grained, planar layer at the Ni interface,
- long, thin, idiomorphic whiskers, and

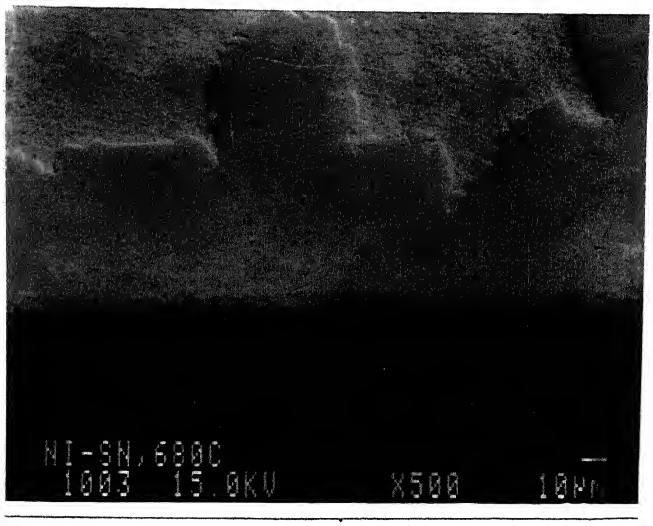

Figure 15: Microstructure of *Ni-Sn* diffusion couple treated at 680^oC for $81h$.

- large, polygonal, idiomorphic crystals.

Next to the Ni_3Sn_4 layer forms the Ni_3Sn_2 layer, which is thin and continuous throughout the interface, with no cracking. The morphology of this layer was found to faceted. Followed by this is a thin dark layer of Ni_3Sn phase. Bottom portion of the micrograph is Ni.

Figure 16 shows the solidified Sn matrix. The needle like precipitates were found to be Ni_3Sn_4 using *Electron Probe Micro Analysis*.

Figure 17 shows the Ni_3Sn_4 crystals present in the Sn matrix at higher magnification.Parts of Ni_3Sn_4 crystals were scrambled off and gets solidified in Sn matrix.These precipitates were found in diffusion couples annealed at each temperatures.

4.2 Growth kinetics of Intermetallics

4.2.1 Growth of Sn rich intermetallic compound Ni_3Sn_4 in the presence of liquid Sn

The Ni_3Sn_4 layer grows by liquid Sn - solid Ni interdiffusion. The saturation of liquid Sn is very fast, because the saturation concentration of the Ni in $Sn(L)$ is

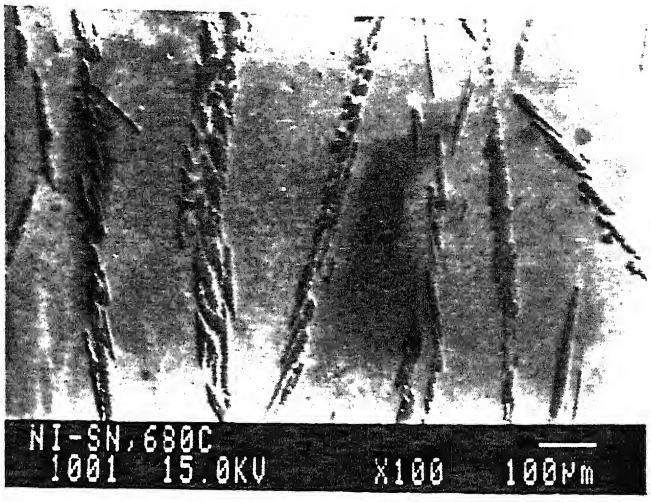

Figure 16: Microstructure showing needle like Ni_3Sn_4 precipitates in the solidified Sn matrix of Ni-Sn diffusion couple treated at $680°C$ for $81h$.

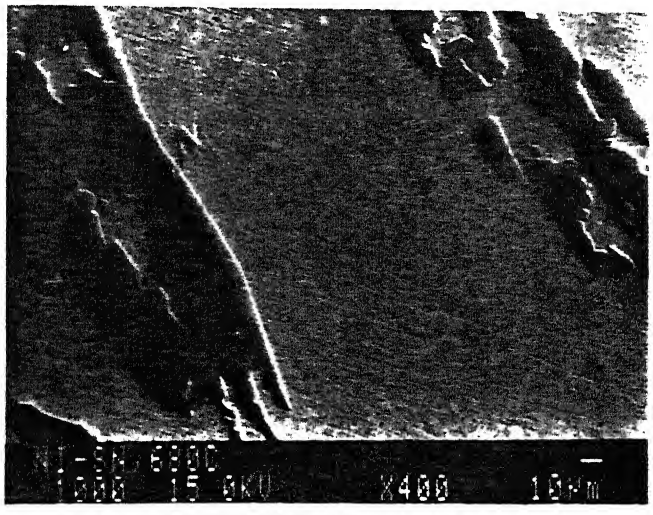

Figure 17: Microstructure showing Ni_3Sn_4 crystals in the solidified Sn matrix at higher magnification of Ni-Sn diffusion couple treated at $680°C$ for $81h$.

very low of the order $1-2wt\%$ at the temperature range $(600°C-700°C)$ we studied. An estimation and measurements by *Toshima et al.* [25] showed that the saturation time is between 1 and 3 *seconds*. The measurement showed that the decrease in the thickness of the Ni at the Ni/Ni_3Sn_4 interface for the intermetallic formation is higher than the penetration depth of Sn in the Ni. So, the border phases are pure Ni and saturated $Sn(L)$.

The growth kinetics of Ni_3Sn_4 layer was studied by measuring the thickness of the layer at the interface.The thickness is measured using Zeiss optical microscope. The hemispherical shape posed problems in measuring the average thickness. We measured the thickness along the interface at specific intervals and the average thickness of this layer was calculated. The measured width of the layer are shown in Table 1.

Average growth distance, $x \times 10^{-5} metres$					
Temperature	*Time (seconds)*				
(^oC)	129600	176400	230400	291600	360000
600	7.26	8.36	9.77	10.88	
620	8.00	9.11	10.99	12.70	14.10
640	8.99	10.20	12.10	13.40	15.04
660	9.90	10.99	12.80	14.00	15.50
680	10.80	11.97	13.90	14.90	16.30
700	11.60	13.00	14.90	16.00	18.60

Table 1: Average growth distance of Ni_3Sn_4 as a function of time and temperature

The diffusion controlled growth of an intermetallic obeys a parabolic growth law given by *Wagner*[27],

$$x = kt^n \tag{15}$$

$$\log x = \log k + n \log t \tag{16}$$

The data are plotted in $\log x$ vs $\log t$ diagram as shown in Figure 18.

As we can see from the diagram there is a linear relationship between $\log x$ and $\log t$.From this plot, the growth exponent n are determined and the results are shown in the Table 2.

Since the n values are close to 0.5, the diffusion of Sn and Ni in the *Ni-Sn* diffusion couple follows the parabolic growth law. The deviation from the parabolic growth is observed at higher temperatures. The reason for the deviation is probably that a large part of transport of the Ni and Sn to the phase boundaries, where the formation of the Ni_3Sn_4 takes place, runs through the grooves between Ni_3Sn_4 crystals. In the

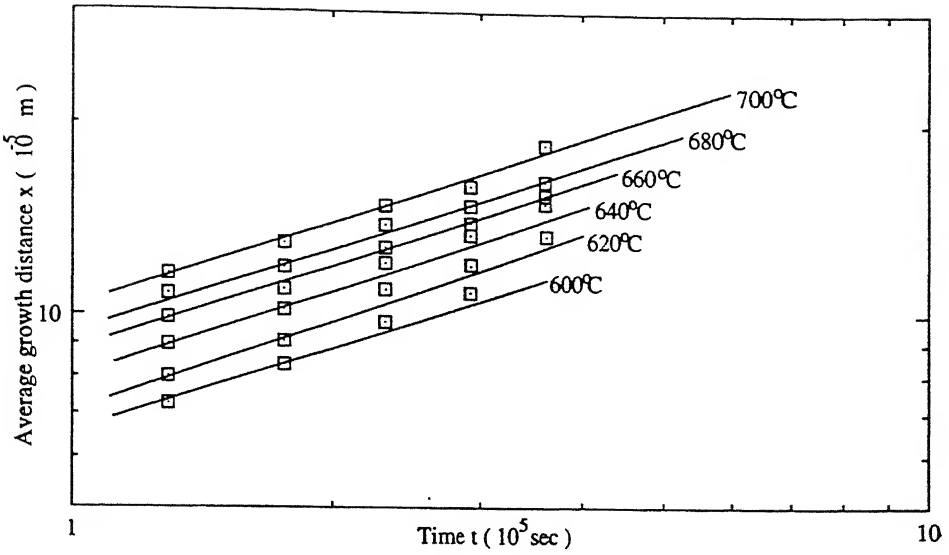

Figure 18: Growth of the Ni_3Sn_4 phase in the temperature range from $600°C$ to $700°C$.

Temperature ($°C$)	n
600	0.4877
620	0.4660
640	0.4452
660	0.4452
680	0.4348
700	0.4244

Table 2: The values of growth exponent n as a function of temperature.

course of time these grooves gets narrower and their density is reduced by a process comparable to grain growth.

Hence, the diffusion slows down. So, from this we can say that the growth velocity is reduced due to three reasons:

1. the increased length of diffusion path.
2. the reduction in concentration gradient.
3. the reduction of transport capacity of the grooves.

In the meantime, other phases Ni_3Sn_2 and Ni_3Sn also start growing. This will also reduce the growth velocity. The growth kinetics of Ni_3Sn_4 layer is studied using the equation

$$k = k_o \exp(-Q/RT) \tag{17}$$

where the penetration constant $k = x^2/t$ is determined by plotting x^2 vs t, Figure 19.

The x^2 values are shown in Table 3.

Square of layer width, $x^2 \times 10^{-9}(metres^2)$					
Temperature	*Time (seconds)*				
(^oC)	129600	176400	230400	291600	360000
600	5.271	6.989	9.545	11.837	
620	6.400	8.299	12.078	16.129	19.880
640	8.082	10.404	14.641	17.956	22.620
660	9.801	12.078	16.384	19.600	24.045
680	11.664	14.328	19.321	22.201	26.567
700	13.456	16.900	22.350	25.600	34.596

Table 3: Square of average growth distance of Ni_3Sn_4 as a function of time and temperature

The k values are shown in Table 4.

Temperature (^oC)	$k \times 10^{-13}$ (m^2/sec)
600	0.411
620	0.511
640	0.620
660	0.690
680	0.790
700	0.920

Table 4: The values of k as a function of temperature.

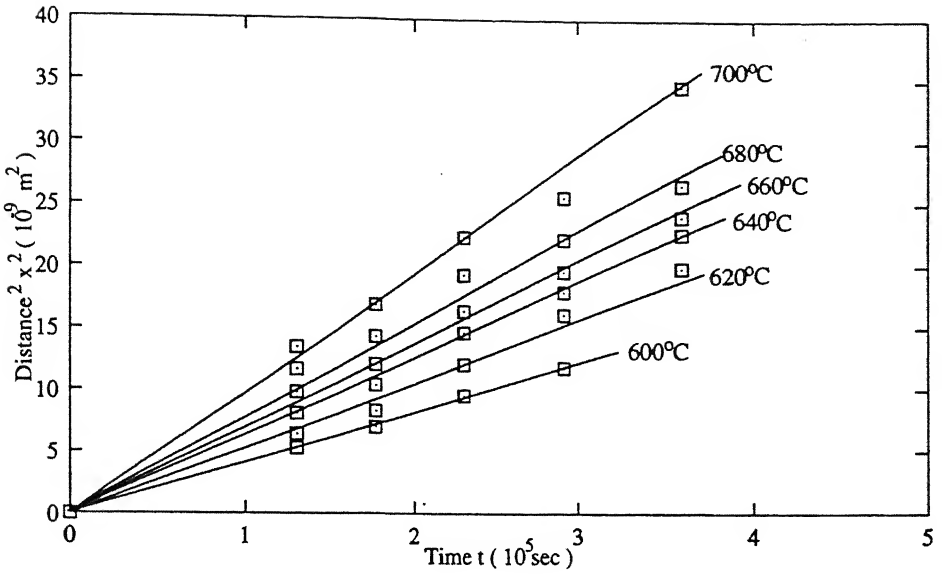

Figure 19: Plot of the square of the layer width of Ni_3Sn_4 phase in the temperature range from $600°C$ to $700°C$.

The penetration constant k is plotted against the reciprocal of absolute temperature $(1/T)$, Figure 20.

The values of k_o and Q are found to be $1.05 \times 10^{-13}\ m^2/sec$ and $53.7\ kJ/mol$, respectively.

We also determined the effective interdiffusion coefficients using the equation given by *Wagner*[27] to compare the activation energy results obtained using a simple relation $x^2 = k\sqrt{Dt}$. The effective diffusion coefficient as given by *Wagner*[27] for the growth of intermetallic layers in binary diffusion couples is,

$$D_{eff} = \frac{(C_{Ni_3Sn_4} - C_{Ni_3Sn_2})\,(C_{Sn} - C_{Ni_3Sn_4})}{\Delta C_{Ni_3Sn_4}\,(C_{Sn} - C_{Ni_3Sn_2})}\,k_p \tag{18}$$

where

- $C_{Ni_3Sn_4}$ is the concentration of Sn in the Ni_3Sn_4 phase,
- $C_{Ni_3Sn_2}$ is the concentration of Sn in the Ni_3Sn_2 phase ,
- C_{Sn} is the concentration of Sn in equilibrium with the Ni_3Sn_4 phase,

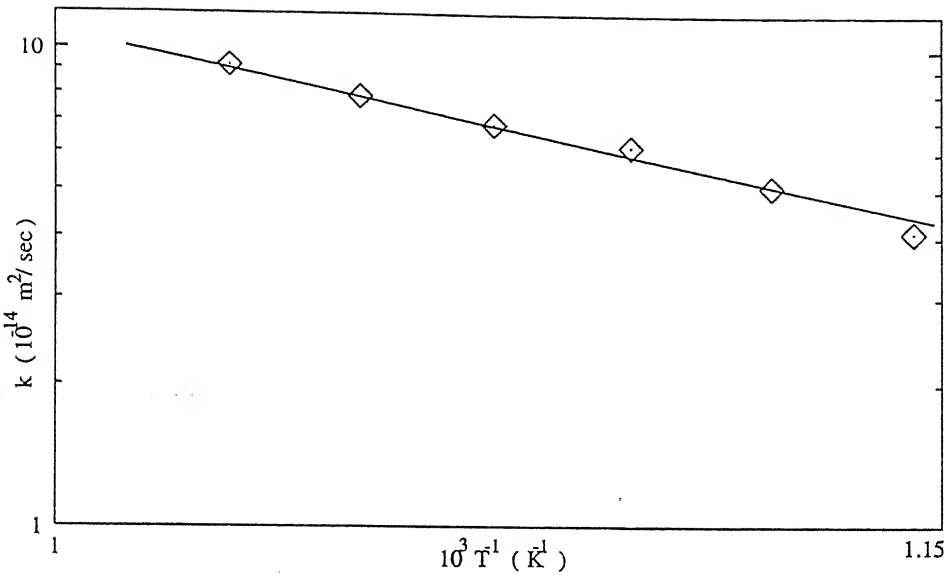

Figure 20: Plot of $\log k$ vs $1/T$ for the Ni_3Sn_4 phase.

- $\Delta C_{Ni_3Sn_4}$ is the homogeneity range of the Ni_3Sn_4 phase in the phase diagram.
- k_p is the parabolic growth constant, which is given by, $k_p = \Delta x^2 \ / \ 2t$.

The concentrations are taken from the *Ni-Sn* phase diagram reported by *P.Nash and A.Nash*[20]. The calculated values of k_p and D_{eff} are shown in Table 5.

Temperature (^oC)	$k_p \times 10^{-13}$ (m^2/sec)	$D_{eff} \times 10^{-13}$ (m^2/sec)
600	0.2330	2.3440
620	0.2651	2.6513
640	0.3273	3.2917
660	0.3496	3.5167
680	0.4000	4.0232
700	0.4769	4.7968

Table 5: The values of k_p and D_{eff} as a function of temperature.

The D_{eff} values were then plotted against $1/T$ as shown in Figure 21 and fitted with the Arrhenius equation.

$$D_{eff} = D^{o}_{eff} \exp\left(-Q_{eff}/RT\right) \tag{19}$$

where R is gas constant and T is temperature in degree kelvin.

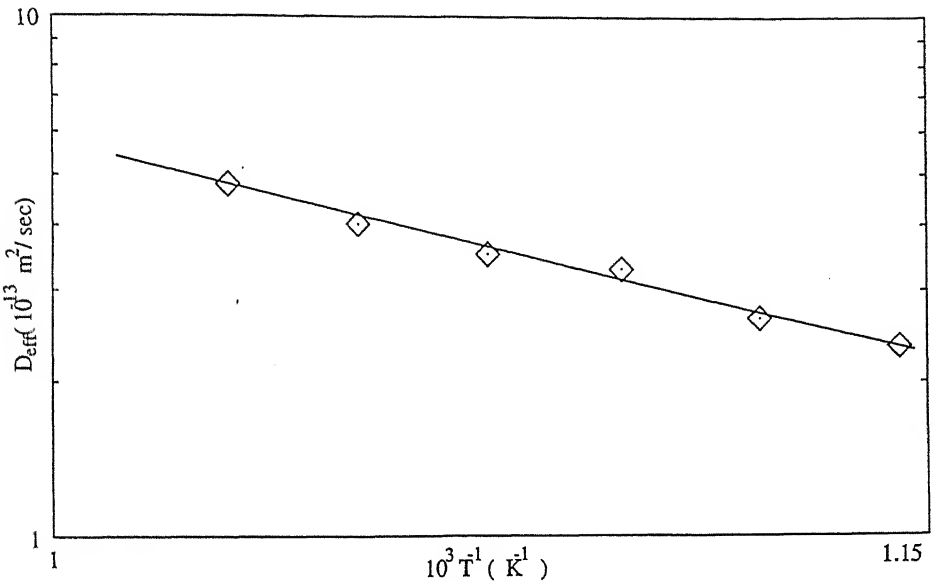

Figure 21: Arrhenius plot of D_{eff} values for the Ni_3Sn_4 phase.

The value of the activation energy determined from the slope of Figure 21 is 50.4 kJ/mol. This value is comparable to the 53.7 kJ/mol obtained from the earlier procedure.

At this point it is appropriate to mention the diffusion mechanism controlling the growth of Ni_3Sn_4 phase in the *Ni-Sn* diffusion couple. Initially, the growth of Ni_3Sn_4 occurs by the diffusion of Ni in liquid Sn as it is in contact. The activation energy of Ni diffusion in $Sn(L)$ is only 19 kJ/mol [19], which is below the value of 53.7 kJ/mol observed in this investigation.

It has been observed that the next intermetallic layer Ni_3Sn_2 although forms initially at the Ni/Ni_3Sn_4 interface, it occupies a uniform layer all along. The groove that formed between Ni_3Sn_4 hemisphere although exists but because of a uniform layer of Ni_3Sn_2, a direct contact between liquid Sn and Ni is lost. Further growth of Ni_3Sn_4 occurs by the diffusion of Ni through Ni_3Sn_2 either in the liquid Sn or in

the Ni_3Sn_4. The growth rate will slow down and the diffusional growth of Ni_3Sn_4 will be controlled by volume diffusion of Ni through Ni_3Sn_2. This may explain a higher activation energy observed for the growth of Ni_3Sn_4 in this investigation.

4.2.2 Growth of Ni rich intermetallic compounds

The Ni_3Sn_2 phase starts growing at the expense of Ni_3Sn_4 and Ni. It started growing as a continuous layer. Its thickness increased with increase in temperature and time.

Earlier *Bader et al.* [1] had shown that there are gaps at the Ni/Ni_3Sn_2 interface and Ni is in direct contact with liquid Sn. However, in this investigation it has been observed that the Ni_3Sn_2 layer is continuous separating Ni_3Sn_4 and Sn from Ni.

The thickness of Ni_3Sn_2 layer was also measured since the layer thickness is relatively small, a higher magnification was used. The data are shown in Table 6.

Average growth distance, $x \times 10^{-6}$ *metres*					
Temperature (^oC)	*Time (seconds)*				
	129600	176400	230400	291600	360000
600	1.60	1.72	1.89	2.03	
620	1.79	1.89	2.03	2.20	2.51
640	2.03	2.31	2.46	2.62	2.97
660	2.70	3.05	3.30	3.48	3.80
680	3.40	3.80	4.20	4.80	5.42
700	4.40	4.98	5.50	6.20	7.20

Table 6: Average growth distance of Ni_3Sn_2 as a function of time and temperature.

The growth distance data are plotted as $\log x$ vs $\log t$ as shown in Figure 22. It shows a linear relationship between x and t. From the diagram we calculated the growth exponent n, and the results are shown in Table 7. This layer also obeys parabolic growth.

The growth exponent n, is observed to increase with increasing temperature and it is approaching parabolic growth. The growth occurs by the diffusion of Ni and Sn through the solid phases, Ni_3Sn_4 and Ni_3Sn_2.

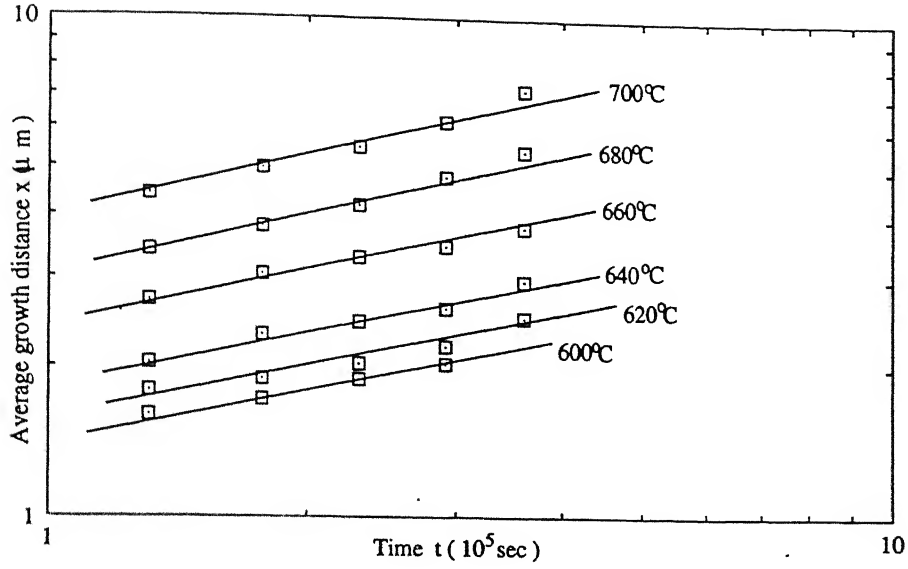

Figure 22: Growth of the Ni_3Sn_2 phase in the temperature range from $600°C$ to $700°C$.

Temperature ($°C$)	n
600	0.404
620	0.404
640	0.412
660	0.418
680	0.424
700	0.424

Table 7: The values of growth exponent n as a function of temperature.

Assuming parabolic growth, the parabolic growth constant k_p is determined using the equation as before.

$$k_p = x^2 \ / \ 2t \tag{20}$$

The calculated results are shown in Table 8.

The effective interdiffusion coefficient D_{eff} were determined using the equation derived by Wagner[27]. At the solid Ni_3Sn_2/Ni_3Sn_4 interface.

Temperature (^oC)	$k_p \times 10^{-17}$ (m^2/sec)
600	0.714
620	0.909
640	1.364
660	2.381
680	4.098
700	6.957

Table 8: The values of k_p as a function of temperature.

$$D_{eff} = \frac{(C_{Ni_3Sn_2} - C_{Ni_3Sn})\,(C_{Ni_3Sn_4} - C_{Ni_3Sn_2})}{\Delta C_{Ni_3Sn_2}\;(C_{Ni_3Sn_4} - C_{Ni_3Sn})}\;k_p \tag{21}$$

where

- C is the mole fraction of Sn.
- $C_{Ni_3Sn_2}$ is the average composition of Sn in Ni_3Sn_2 phase.
- C_{Ni_3Sn} is the composition of Sn in Ni_3Sn phase.
- $C_{Ni_3Sn_4}$ is the composition of Sn in Ni_3Sn_4 phase and
- $\Delta C_{Ni_3Sn_2}$ is the homogeneity range of the Ni_3Sn_2 phase.

The concentrations are taken from the $Ni - Sn$ phase diagram reported by *P. Nash and A.Nash*[20]. The computed D_{eff} values are shown in Table 9.

The D_{eff} values are plotted against $1/T$ as shown in Figure 23 and fitted with an Arrhenius equation.

$$D_{eff} = D^o_{eff}\;\exp\,(-Q_{eff}/RT) \tag{22}$$

The value of the activation energy determined from the straight line is 206 kJ/mol.

In one of the earlier investigation *Bader et al.*[1] reported the growth of Ni_3Sn_2 layer by grain boundary diffusion. However, since no grain boundaries are observed in the microstructure of Ni_3Sn_4, the growth of Ni_3Sn_2 by grain boundary diffusion

Temperature (^oC)	$D_{eff} \times 10^{-16}$ (m^2/sec)
600	0.156
620	0.202
640	0.303
660	0.529
680	0.911
700	1.545

Table 9: The values of D_{eff} as a function of temperature.

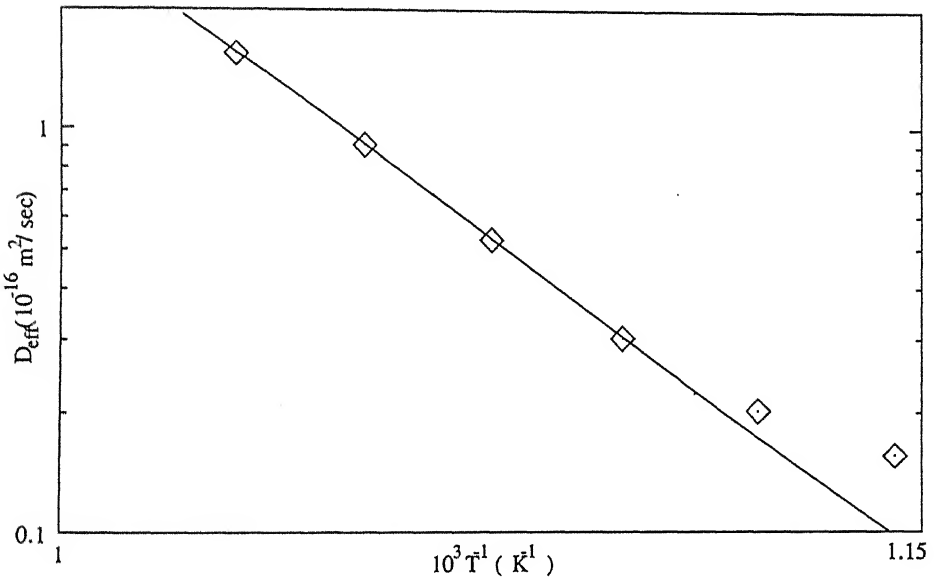

Figure 23: Arrhenius plot of D_{eff} values for the Ni_3Sn_2 phase.

can be ruled out. The activation energy obtained for the growth of Ni_3Sn_2 can be associated with the volume diffusion of Ni through Ni_3Sn_2 or Sn through Ni_3Sn_4 whichever is slower and rate controlling.

In order to verify the results, we also plotted x^2 and t values as shown in the Figure 24 to first determine k values from the relation,

$$k = x^2 \ / \ t \tag{23}$$

The x^2 values are shown in Table 10.

Square of layer width, $x^2 \times 10^{-12}$ $(metres^2)$					
Temperature	*Time (seconds)*				
(^oC)	129600	176400	230400	291600	360000
600	2.560	2.958	3.572	4.121	
620	3.204	3.572	4.121	4.840	6.300
640	4.121	5.336	6.052	6.864	8.821
660	7.290	9.303	10.890	12.110	14.440
680	11.560	14.440	17.640	23.040	29.376
700	19.360	24.800	30.250	38.440	51.840

Table 10: Square of average growth distance of Ni_3Sn_2 as a function of time and temperature.

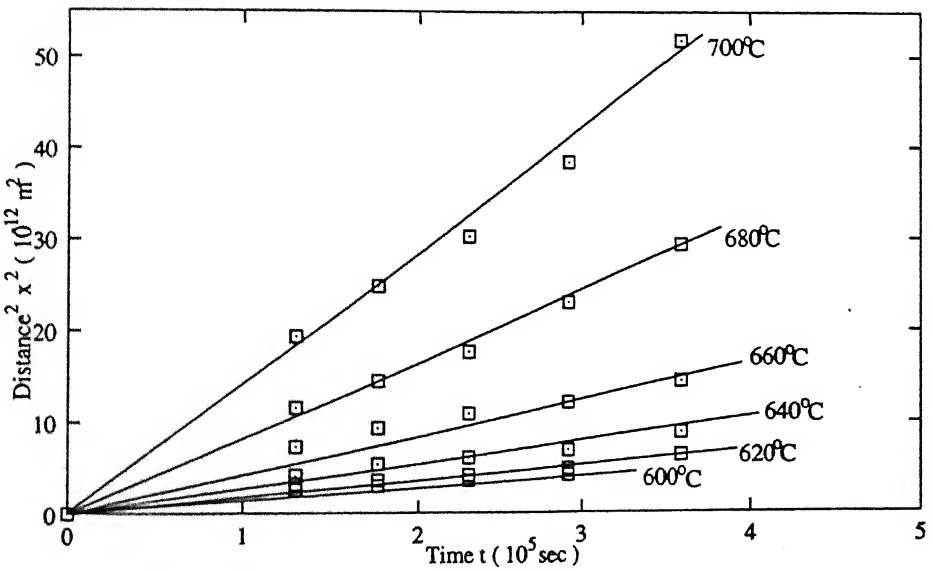

Figure 24: Plot of the square of the layer width vs time for the Ni_3Sn_2 phase in the temperature range between 600^oC and 700^oC.

The values of k determined from the Figure 24 are shown in Table 11.

The penetration constant k is fitted with the equation

$$k = k_o \, exp \, (-Q/RT) \tag{24}$$

Temperature (^oC)	$k \times 10^{-16}$ (m^2/sec)
600	0.144
620	0.177
640	0.266
660	0.472
680	0.800
700	1.400

Table 11: The values of k as a function of temperature.

as shown in Figure 25.

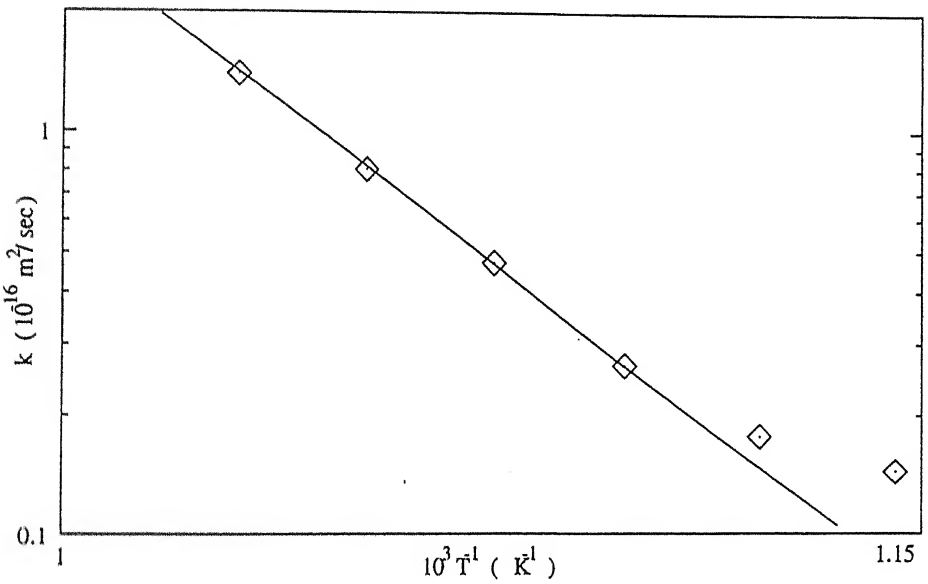

Figure 25: Plot of $\log k$ vs $1/T$ for the Ni_3Sn_2 phase.

The values of k_o and Q are found to be 1.9 $\times$ 10^{-16} m^2/sec and 208.1 kJ/mol, respectively. The value of the activation energy agrees with that determined using D_{eff} values.

The activation energy determined by *Vanbeek et al.*[26] for the diffusion of Sn in Ni in the temperature range between 709^oC and 793^oC is 244 kJ/mol.

The activation energy for the volume diffusion of Sn in solid Ni is 248.4 kJ/mol [15].

Our value although lower by about 40 kJ/mol falls in the same range and therefore the growth of Ni_3Sn_2 phase can be associated with the volume diffusion.

In Ni_3Sn/Ni_3Sn_4 diffusion couples, using markers *Vanbeek et al.* [26] studied the interface migration. They found the *Kirkendall interface* close to Ni_3Sn side, dividing the Ni_3Sn_2 layer in about 1 : 2 ratio. They also found the D_{Ni}/D_{Sn} ratio to be 4 $\times$ $\overline{V}_{Ni}$ / $\overline{V}_{Sn}$. Hence, from this Ni is the most mobile element.

In the case of Ni_3Sn layer it became difficult to measure the layer thickness since it was observed to be very small. From the morphology it can be mentioned that Ni_3Sn phase also grows through solid state diffusion. Here also, Ni is reported to be the most mobile element. Using marker experiments *Vanbeek et al.* [26] have shown that the D_{Ni}/D_{Sn} value is equal to 40 $\times$ $\overline{V}_{Ni}/\overline{V}_{Sn}$.

4.3 Concentration Distance Profile

The concentrations of Sn and Ni were measured at the interface using *Electron Probe Micro Analyzer*. The results are plotted in Figures (26 -31).

Figure 26 shows the Sn concentration as a function of distance from the pure Ni end of the Ni-Sn diffusion couple treated at 600^oC for 81 *hours*.

The left hand end is Ni rich where concentration of Sn is very low, of the order of $0-2$ *atom* %. The Ni_3Sn phase is just a few microns thick. The Ni_3Sn_2 phase is formed next whose thickness is relatively large. The Sn concentration in the Ni_3Sn_4 layer is in the range of $52-56$ *atom* %. The last layer is a saturated solid solution of Ni in Sn.

Figure 27 shows the concentration - distance profile for the diffusion couple treated at 620^oC for 100 *hours*. The Ni_3Sn_2 phase forms as a continous layer and Ni_3Sn layer is also found to be grown.

Figures (28 - 31) show the concentration - distance profiles for the diffusion couples treated at 640^oC, 660^oC, 680^oC and 700^oC for 100 *hours* respectively. As the temperature increases, the layer thickness increases. The Sn concentration is observed to be equal at higher temperature in the respective intermetallic phases.

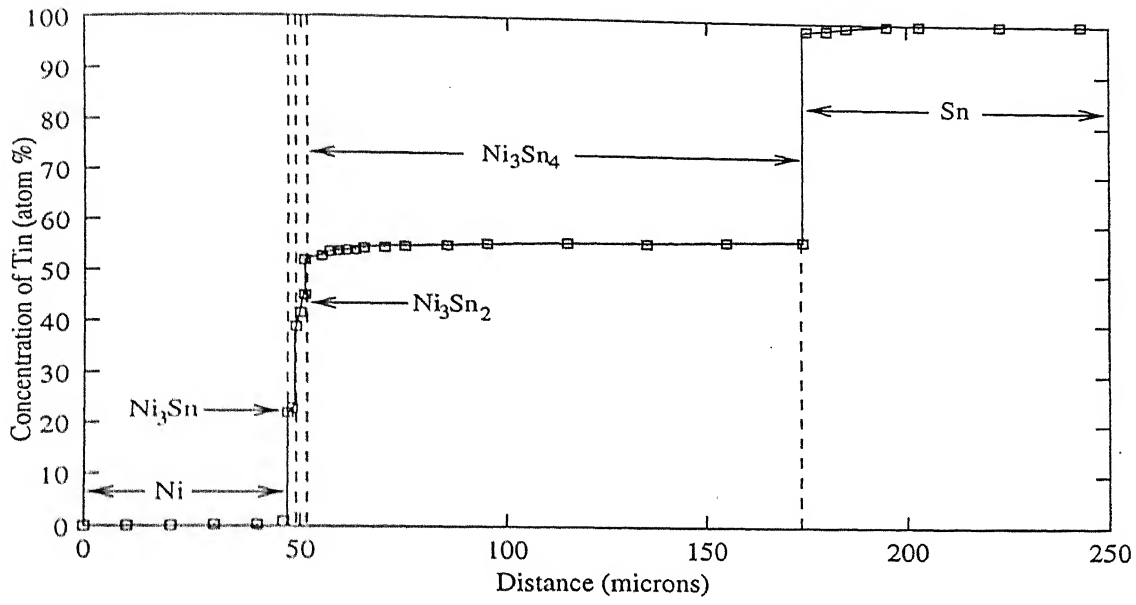

Figure 26: Concentration - distance profile for the *Ni-Sn* diffusion couple treated at 600^oC for 81 *hours*.

From the concentration - distance profiles, the values of phase boundary concentrations at different temperatures are noted and the results are plotted as shown in Figure 32.

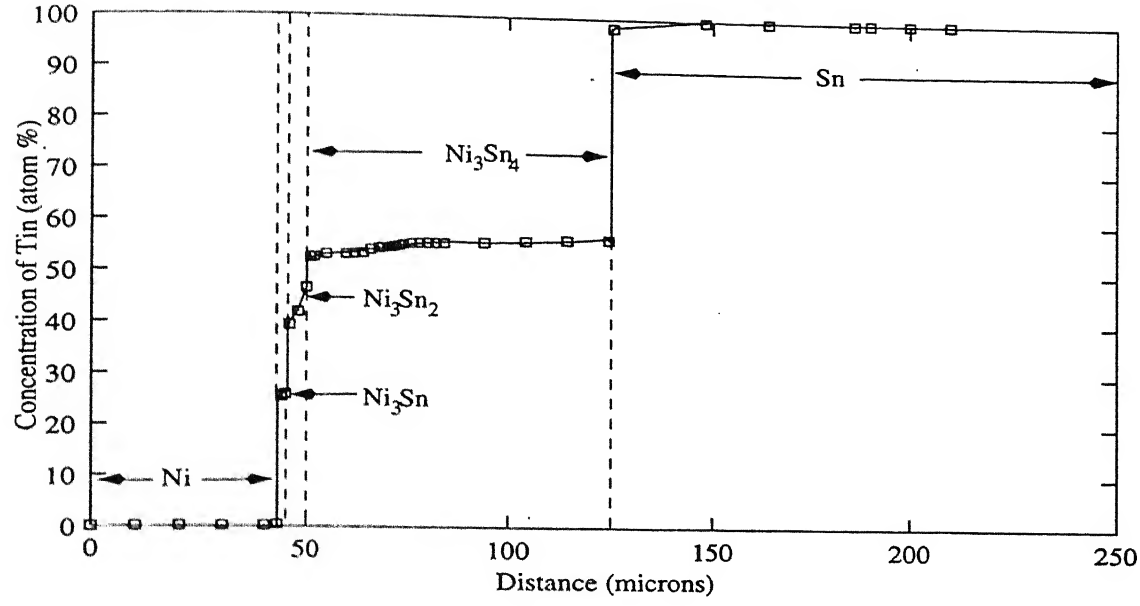

Figure 27: Concentration - distance profile for the *Ni-Sn* diffusion couple treated at $620°C$ for 100 *hours*.

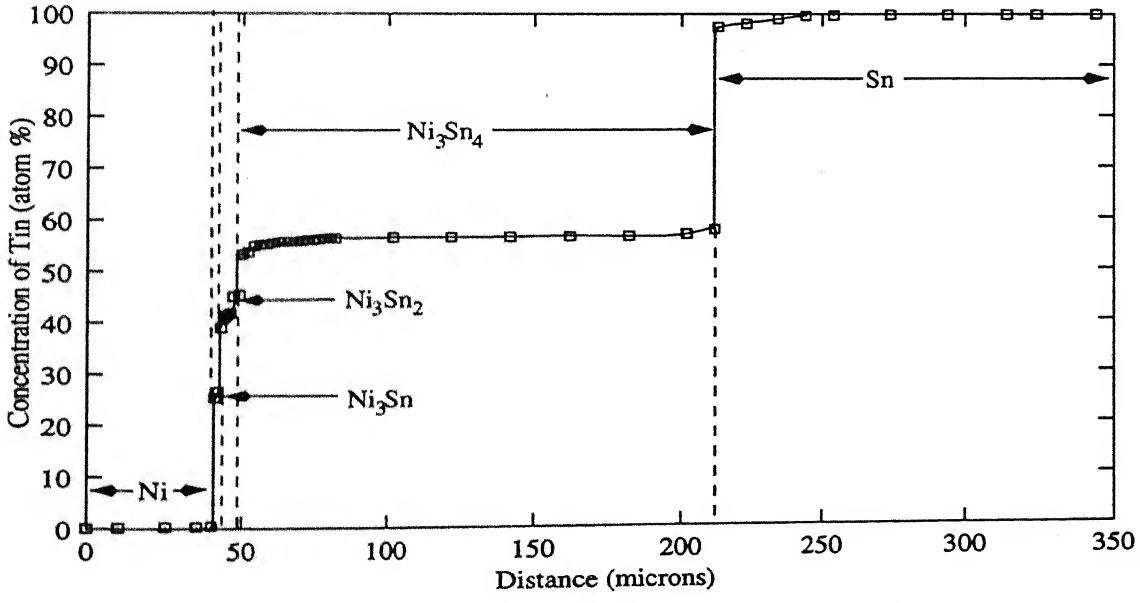

Figure 28: Concentration - distance profile for the *Ni-Sn* diffusion couple treated at $640°C$ for 100 *hours*.

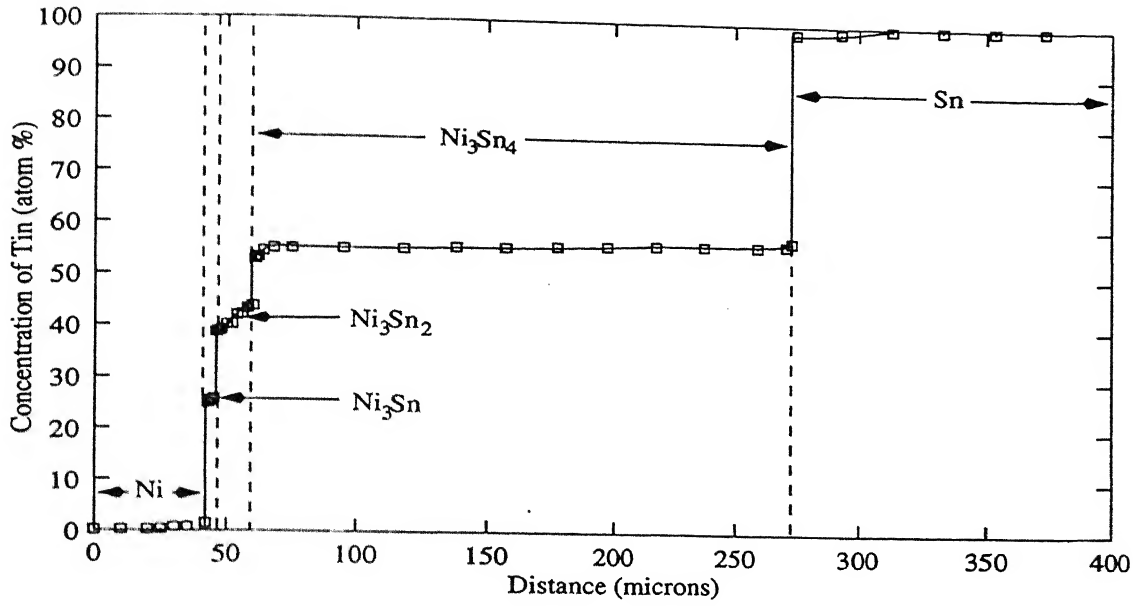

Figure 29: Concentration - distance profile for the *Ni-Sn* diffusion couple treated at $660°C$ for 100 *hours*.

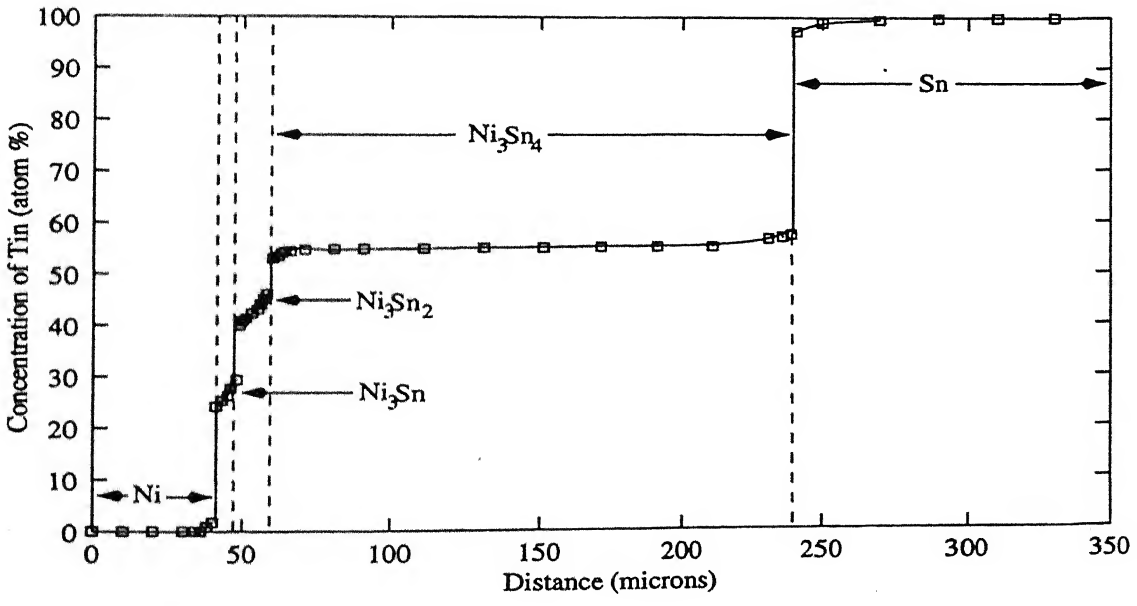

Figure 30: Concentration - distance profile for the *Ni-Sn* diffusion couple treated at $680°C$ for 100 *hours*.

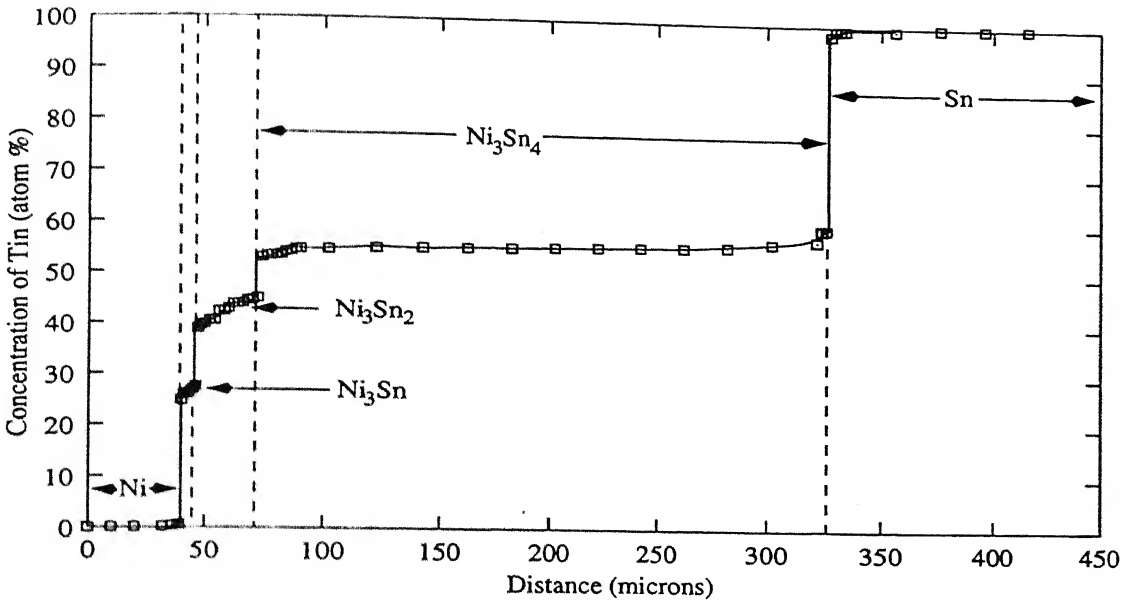

Figure 31: Concentration - distance profile for the *Ni-Sn* diffusion couple treated at $700°C$ for 100 *hours*.

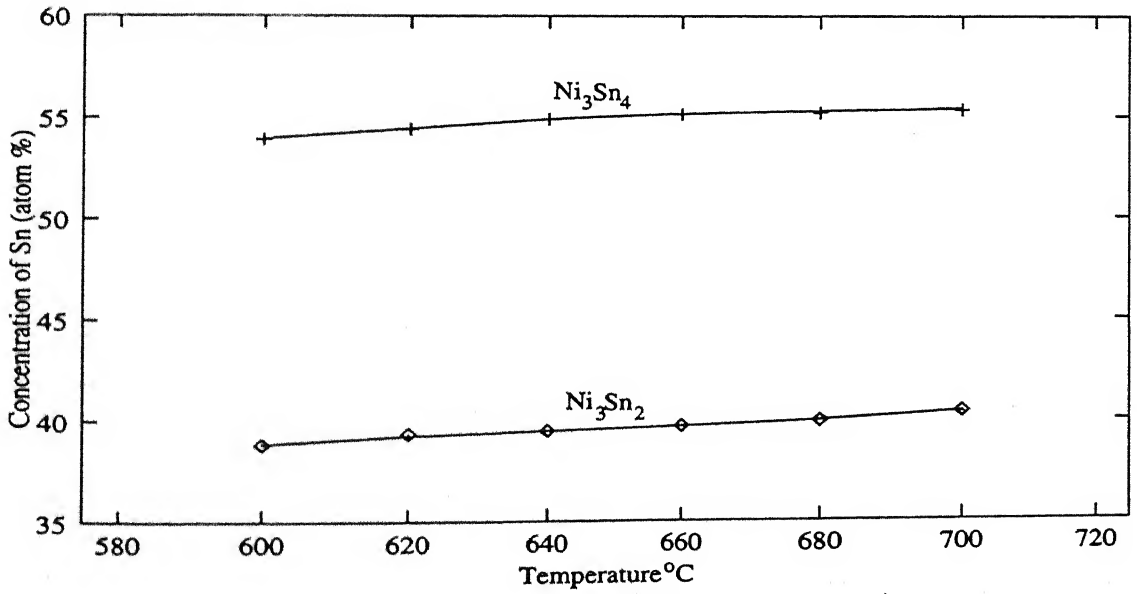

Figure 32: Phase boundary concentrations of *Ni-Sn* diffusion couples as a function of temperature.

Chapter 5

Conclusion

The experiments in the *Ni-Sn* system led to the following results :

1. In the diffusion couples all layers, which can be expected on the basis of the *Ni-Sn equilibrium phase diagram*, are indeed present in the diffusion zone.

2. The morphology of the intermetallic layer was found to be faceted.

3. The layer growth of Ni_3Sn_4, Ni_3Sn_2 and Ni_3Sn in the diffusion couples obeys the parabolic growth law, indicating volume diffusion mechanism.

4. Initially, the growth of Ni_3Sn_4 occurs by the diffusion of Ni in liquid Sn. Later, due to the formation of Ni_3Sn_2, the growth gets slowed and further growth of Ni_3Sn_4 occurs by the diffusion of Ni through solid Ni_3Sn_2 layer.

5. For the growth of Ni_3Sn_2 and Ni_3Sn, the calculated activation energies were close to volume diffusion data, indicating the bulk diffusion process.At temperatures below $640°C$, the low value of activation energy was found. This is due to the diffusion of liquid Sn through grooves between Ni_3Sn_4 hemispheres.

6. The composition range of Ni_3Sn_4 and Ni_3Sn_2 determined from the concentration - distance profiles agrees well with that of equilibrium diagram.

Bibliography

[1] BADER, S., ET AL. Rapid Formation of Intermetallic Compounds by Interdiffusion in the Cu-Sn and Ni-Sn Systems. *Acta Metallurgica.et. Materialia. 43*, 1 (1995), 329–337.

[2] BEKE, D. L., AND SZABÓ, I. A. Effect of Stress on Diffusion. *Defect and Diffusion Forum 95-98* (1993), 537–554.

[3] DEAL, B. E., AND GROVE, A. S. General Relationship for the Thermal Oxidation of Silicon. *J. Applied Physics 36*, 12 (Dec 1965), 3770–3778.

[4] DESRÉ, P. J., AND YAVARI, A. R. Homogeneous Nucleation via Atomic Density Fluctuations in Undercooled Liquid Metals. *J. Alloys Comp.* (1992).

[5] D'HEURLE, F. M. Nucleation of New Solid Phases from Chemical Interactions at an Interface. *J. Vacuum Science and Technology A.7*, 3 (May-Jun 1989), 1467–1471.

[6] DYBKOV, V. I. Reaction Diffusion in Heterogeneous Binary Systems part 1. *J. Materials Science 21* (1986), 3078–3084.

[7] DYBKOV, V. I. Reaction Diffusion in Heterogeneous Binary Systems part 2. *J. Materials Science 21* (1986), 3085–3090.

[8] DYBKOV, V. I. Reaction Diffusion in Heterogeneous Binary Systems part 3. *J. Materials Science 22* (1987), 4233–4239.

[9] EVANS, U. R. *An Introduction to Metallic Corrosion.* Edward Arnold Publishers, London, 1981.

[10] GAS, P., AND D'HEURLE, F. M. Formation of Intermediate Phases , Ni_3Si_2 and Pt_6Si_5 : Nucleation , Identification and Resistivity. *J. Applied Physics 59*, 3 (May 1986), 3458–3466.

[11] GÖSELE, U. *In Alloying.* J. L. Walter and M. Jackson , ASM International, 1988.

[12] GÖSELE, U., AND TU, K. N. Growth Kinetics of Planar Binary Diffusion Couples Thin-film case versus Bulk cases. *J. Applied Physics 53*, 4 (Apr 1982), 3252–3260.

[13] GUSAK, A. M., AND GUROV, K. P. Peculiarities of Intermediate Phase Nucleation in the Process of Chemical Diffusion. *Diffusion and Defect Data, Solid State B, Solid State Phenomena 23-24* (1992), 117–122.

[14] KANG, S. K., AND RAMACHANDRAN, K. Growth Kinetics of Intermetallic Phases at the Liquid Sn and Solid Ni Interface. *Scripta Metallurgica* (Apr 1980), 421–424.

[15] KAUR, I., AND GUST, W. *Handbook of Grain and Interphase Boundary Diffusion Data*, vol. 2. Ziegler Press, Stuttgart, Germany, 1989.

[16] KHEDER, A. R. I., AND GREENWOOD, G. W. Some Characteristics of Porosity arising because of the Kirkendall effect. *Defect and Diffusion Forum 95-98* (1993), 573–578.

[17] KIDSON, G. V. Some aspects of the Growth of Diffusion Layers in Binary Systems. *J. Nuclear Materials 3*, 1 (1961), 21–29.

[18] KIRKENDALL, E. D., AND SMIGELSKAS, A. D. Zinc Diffusion in Brass. *Trans. AIME 171* (1947), 130–142.

[19] MA, C. H., AND SWALIN, R. A. A Study of Solute Diffusion in Liquid Tin. *Acta Metallurgica 8* (Jun 1960), 388–395.

[20] MASSALSKI, T. B., ET AL., Eds. *Binary Alloy Phase Diagrams.* ASM Int., Materials Park, Ohio, 1989.

[21] NEUHAUS, P., AND HERZIG, C. Temperature Dependence of the Grain Boundary Diffusion of Tin in Nickel. *Acta Metallurgica 35*, 4 (1987), 881–886.

[22] PHILIBERT, J. Reactive Diffusion. *Defect and Diffusion Forum 66-69* (1989), 995–1014.

[23] REEDHILL, R. E. *Physical Metallurgy Principles.* Van Nostrand Reinhold, Newyork, 1964.

[24] STEPHENSON, G. B. Diffusion Induced Flow and Stress during Interdiffusion in Amorphous Systems. *Defect and Diffusion Forum 95-98* (1993), 507–520.

[25] TOSHIMA, S., ET AL. Saturation Time Measurements. *RCA (Radio Corporation of America) Review 45* (Mar 1984), 90.

[26] VANBEEK, J. A., ET AL. Multiphase Diffusion in the systems Fe-Sn and Ni-Sn. *Z. Metallkde.* (Jul 1982), 439–444.

[27] WAGNER, C. The evaluation of data obtained with Diffusion Couples of Binary Single-phase and Multi-phase Systems. *Acta Metallurgica 17* (Feb 1969), 99–108.